Thesis for the degree of doctor of philosophy (PhD)

The lateralmost aspect of the superficial dorsal horn and the lateral spinal nucleus (LSN) of the lumbar spinal cord of the rat: anatomical description of neurons and electrophysiological study of their propriospinal connections

by Zsófia Antal, MD

Supervisor: Péter Szücs, MD, PhD

UNIVERSITY OF DEBRECEN

DOCTORAL SCHOOL OF NEUROSCIENCES

Debrecen, 2015

TABLE OF CONTENTS

ABBREVIATIONS AND ACRONYMS

AC – anterior commissure
ACSF – arteficial cerebrospinal fluid
ALT – anterolateral tract
AP – action potential
ASIC – acid-sensing ion channel
BDA - biotinylated dextran amine
BMP7 – bone morphogenetic protein 7
c-ALT – contralateral anterolateral tract
CCD – charge coupled device
CGRP – calcitonin gene-related peptide
CGRP – calcitonin gene-related peptide
CIP – congenital insensitivity to pain
DAB – diaminobenzidine
DCT – dorsal collateral type
DF – dorsal funiculus
DH – dorsal horn
DIC –differetial interference contrast microscpy
DLF – dorsolateral funiculus
DLF – dorsolateral funiculus
DRG – dorsal root ganglion
EPSC – excitatory postsynaptic current
EPSP – excitatory postsynaptic potential
FRAP - fluoride-resistant acid phosphatase
GABA - gamma-aminobutyric acid
GAL - galanin
GDNF - glial cell line-derived neurotrophic factor
HIV – human immunodeficiency virus
HRP-DAB – horseradish peroxidase - diaminobenzidine
i-ALT – ipsilateral anterolateral tract
i-DF – ipsilateral dorsolateral funiculus
i-DLF – ipsilateral dorsolateral funiculus
IB4 - Griffonia Simplicifolia B4 isolectin
IR-LED – infrared light emitting diode
L-I – lamina I
lamina Iii – the inner one-third of lamina II
lamina IIo - the outer two-third of lamina II
LCN – local circuit neuron
LCT – lateral collateral type
LF – lateral funiculus
LI-X – lamina I-X

LSN – lateral spinal nucleus
MCT – mixed collateral type
MrgprD - Mas-related G-protein coupled receptor member D
NGF – nerve growth factor
NK1 – neurokinin 1
nNOS - neural nitric oxyd synthase
NON-N – non-nociceptive neuron
NPY - neuropeptide Y
NS – nociceptive specific
NSAID – non-steroid anti-inflammatory drug
OUT – neuron between the lateral edge of the dorsal grey and the LSN
$P2X_3$ - P2X purinoceptor 3
PC – posterior commissure
PN – projection neuron
PV - parvalbumin
SEM – standard error of the mean
sEPSC – spontaneous excitatory postsynaptic current
sEPSP – spontaneous excitatory postsynaptic potential
SP – substance P
TrkA - Tropomyosin receptor kinase A
TRPA1 - Transient receptor potential cation channel, subfamily A, member 1
TRPM8 - Transient receptor potential cation channel subfamily M member 8
TRPV1 – transient receptor potential cation channel subfamily V member 1
VCT – ventral collateral type
VIP – vasoactive intestinal peptide
WDR – wide dynamic range neuron

INTRODUCTION

The unpleasant sensation of pain is an experience that almost all of us have already encountered. Pain can be superficial or deep, pricking, burning, lancinating or dull, but it is definitely something everyone tries to avoid. However, in the rare cases of congenital insensitivity to pain (CIP), patients who fail to perceive painful stimuli are surprisingly vulnerable, and their disease can have fatal consequences. This phenomenon can be explained by the evolutionary origin of pain, as it is assigned to alarm the body about the danger situation, which potentially causes tissue damage. Those harmful stimuli, which threaten the integrity of the organism, from high temperature and mechanical insults to chemical irritants, are called noxa, while the process, during which the central nervous system encodes the noxious stimulus to the perception of pain, is referred to as nociception *(www.iasp-pain.org/Taxonomy)*. While pain in some terms is similar to other sensory processes, it also provokes a series of behavioural, autonomic and endocrine responses, it has a very strong learning impact and in some pathologic cases it can remodel one's personality, therefore the concept of nociception seems to be more complex than that of other senses *(Basbaum and Bushnell 2009)*. When someone touches a hot pan, he will reflexively retract his hand, and he will immediately and unconsciously flex his lower limb when stepping onto a nail. This so-called flexor reflex provides a defence mechanism against the noxious thermal and mechanical stimuli mentioned above, while one will be aware of the harm, and will try to avoid contacting the noxa in future. The driving force behind these events is the unpleasant sensation of pain. This type of nociceptive pain results from the processing of a brief noxious stimulus and, as it is assigned to guard tissue integrity, is sometimes referred to as "good" or "useful" pain.

While nociceptive pain arises from the normal function of the somatosensory system, neuropathic pain is elicited by pathological processes affecting the nociceptive system itself. It can be regarded as a maladaptive condition, since there is no adequate stimulus in the background *(McMahon and Koltzenburg 2006)*. As the provoking factor often persists, it is mostly a chronic state in contrast to nociceptive pain, which is rather acute. The damaged neural elements are characterized by an abnormal function, which results in spontaneous pain, pain elicited by normally non-painful stimulus (allodynia), or pain provoked by lower

stimulus intensity than in normal cases and increased pain reaction to suprathreshold stimuli (hyperalgesia) *(Basbaum and Bushnell 2009)*. These severe chronic symptoms not only seriously worsen the quality of life, but also often distort the personality. As neuropathic pain often accompanies stroke, multiple sclerosis, spinal cord injuries, diabetes mellitus, HIV infection or different types of cancer *(Szirmai, 2006)* it affects millions of patients worldwide.

Relieving pain has been a mission of medicine from the beginning of times. It is important during the treatment of any kind of disease because it increases the patient's well-being, improves his cooperation and makes surgical interventions possible. Moreover, in terminal illnesses soothing pain can be the only thing a doctor can do for his patient. Nonetheless, after several scientific revolutions, in the age of modern technology, finding the ideal analgesic remains a challenge, as it should meet several requirements at the same time. It should selectively decrease nociception, while leaving the other sensory processes intact. It should have no influence either on the state of mind or on the ability to work. It should have a wide therapeutic index and no side effects. Last but not least, it should be cheap and easy to dose orally. *(Fürst, 2006)* Among the wide range of available analgesics, opioids are the oldest in use and still regarded as gold standard in the treatment of chronic pain, despite the fact that beside their acknowledged pain relieving effect their sedative impact and abuse potential is not negligible. During the past decades several alternatives have been suggested for opioids, although in most of the cases they didn't prove as effective as opioids and gained clinical recognition only in specific therapeutic fields, like the antidepressant amitriptylin in postherpetic neuralgia or the anticonvulsant carbamazepine in trigeminal neuralgia. As our knowledge about the pronociceptive effects of prostaglandins is expanding, the non-steroid anti-inflammatory drugs (NSAIDs) cannot be regarded as solely peripheral analgesics anymore, therefore they might gain new therapeutic applications in the future. At the same time there is also intensive on-going research focusing on the endocannabinoid system and the potential clinical use of cannabinoids in analgesic therapy *(McMahon and Koltzenburg, 2006*).

To move forward in the improvement of analgesics, it is indispensable to expand our knowledge about the nociceptive system itself. The better we understand the sensory processing of the painful stimulus from the peripheral nociceptor to the central nervous system, the more possibilities we have to intervene. In this

information processing the spinal cord has long been thought to act as a relay station, which simply mediates the stimulus from the periphery to the central nervous system. However, today we already know that its role is much more complex than that. It performs the primary coordinative, regulatory and modulatory function in nociception. Since 1965, when Melzack and Wall proposed their gate-control theory *(Melzack and Wall, 1965),* an increased attention has turned to the action of the eventual neural circuitry located in the spinal dorsal horn. Getting to know the specific neural populations in the spinal dorsal horn, describing their neurochemical and electrophysiological properties can lead to a better understanding of the complex operation of neural circuits in the spinal dorsal horn and their precise role in nociceptive information processing. Such knowledge would be fundamental to develop specific and effective analgesics, which lack supraspinal side effects.

THEORETICAL BACKGROUND

Overview of the nociceptive system's anatomy

Regarding the theoretical debates about the essential of pain, two controversial approaches are opposing each other. According to specificity theory, developed by Charles Bell *(Bell and Shaw, 1868)* each sensory modality is a result of the activation of a specific neural population. The pattern theory (*Sinclair, 1955; Weddel, 1955),* on the other hand, states that different sensory modalities may arise from different activation patterns of a non-specific neural network. This apparently philosophical question has a strong influence on the practical aspects of pain-research. If we recognise pain as a specific sensory modality, the neural substrates responsible for it has to be identified *(Basbaum and Bushnell, 2009).* Although in reality the specificity and pattern theories are completing each other, there is a mass of research data proving that there exist specific sensory receptors in the skin, joints and viscera, the activation of which results in the sensation of pain *(Belmonte and Cervero, 1996).*

These receptors are called nociceptors, because their adequate stimuli are noxae, those harmful effects on the body, which threaten tissue integrity *(Sherrington, 1906)*. Nociceptors can be categorized according to four properties: 1) level of myelination, 2) stimulus modality, which evokes response, 3) response characteristics and 4) distinctive neurohistochemical markers *(McMahon and Koltzenburg 2006).*

Most of the primary afferent fibres, which supply nociceptors, are either medium diameter (2-6 μm), myelinated Aδ fibers with a conduction velocity of 12-30 m/s, or small diameter (0.4-1.2 μm), unmyelinated C fibers with a conduction velocity of 0.5-2 m/s *(Millan, 1998)*. While the first group is considered mediating fast, well-localized, sharp or "first pain", the second group is probably responsible for poorly localized, slow, dull or "second pain" *(Millan, 1998; Basbaum, 2009)*. It has to be noted, however, that both in the Aδ and C group there are fibers, which convey non-nociceptive information and, in addition, the thick myelinated Aβ fibers, which convey low intensity mechanical stimuli under normal conditions, can become sensitive to noxious stimulation in case of tissue or nerve injury. It has also been reported that Aβ fibers may also contribute to the transmission of nociceptive information from muscle (*Mense, 1993*). In terms of the adequate stimulus, some nociceptors are responsive exclusively to mechanical, thermal or chemical stimuli,

while others are responsive to the combination of two or three, the latter often mentioned as polymodal nociceptors *(Willis and Coggeshall, 2004)*. According to the results of electrophysiological studies, most of the Aδ fibers are polymodal and can be subdivided into Type I and Type II nociceptors, being susceptible to mechanical and chemical stimuli with a heat threshold above 50 °C or having low heat and high mechanical threshold, respectively (*Handwerker and Kobal, 1993; Simone and Cajander, 1997; Treede and Magerl, 1995; Millan, 1998; Basbaum, 2009*). C fibers are also heterogeneous and most of them are polymodal, including a group of mechanical and heat responsive nociceptors (*Millan, 1998; Perl, 2007; Basbaum et al., 2009*). While the threshold of nociceptors can be a discrete value, in some cases they are characterized by a progressive discharge pattern and show the highest response when the stimulus becomes damaging *(Willis and Coggeshall, 2004*). There is also a group of silent nociceptors, which are normally irresponsive to noxious stimuli unless they are sensitized by an occurring tissue injury or inflammation, and become responsive to a range of chemical mediators *(Reeh et al., 1987; Koltzenburg, 1995; Millan, 1998)*. Nociceptors can also be classified according to their expression of different markers, which indicate their sensitivity to heat (TRPV1), cold (TRPM8), acidic pH (ASICs) chemical irritants (TRPA1) and mechanical stimuli (MrgprD) (*Julius and Basbaum, 2001; Cavanaugh et al., 2009; Basbaum, 2009; Knowlton et al., 2013;, Braz et al., 2014*).

Regarding their anatomical structure, cutaneous nociceptors are free nerve endings of primary afferent fibres protruding into the epidermis of the skin. These fibres are the peripheral axonal processes of primary sensory neurons in the dorsal root ganglion (DRG) in case of afferents from the body, and in the trigeminal ganglion in case of the afferents from the face (*Réthelyi, 2002*). Primary sensory neurons are pseudo-unipolar, possessing a short axonal stalk that bifurcates to a peripheral and to a central terminal (*Réthelyi, 2002*). While the free nerve endings of the peripheral processes form the above-mentioned nociceptors, the central process enters the spinal cord and establishes synaptic connections with the secondary sensory neurons in the spinal dorsal horn. Neurons of the DRG are generally classified on the basis of their soma size and it's staining with basic analyne dyes (*Nissl, 1894; Cajal, 1909*). Those neurons, that contain high amount of neurofilament, stain light with the regular basic dyes, but can be made visible with RT97, a specific phosphorylated 200-kD neurofilament antibody *(Lawson and Waddel, 1991)*.

Although their soma size can show some variety, it is rather large, therefore these neurons are traditionally mentioned in the literature as large light cells. This population gives rise to myelinated axons, which conduct in the Aβ and in the Aδ range. On the other hand, darkly stained cells are usually uniformly small and they are associated with both C and Aδ fibers *(Harper and Lawson, 1985)*. In terms of function one can distinguish high-threshold responder nociceptive and low-threshold responder non - nociceptive sensory neurons in the DRG. Although oversimplified, there is a certain degree of correlation between morphology and function of these neuronal groups, in a way that small dark cells are traditionally regarded being involved in nociception and large light cells are accepted as non-nociceptive *(Willis and Coggeshall, 2004)*. Those small dark cells, which give rise to C fibers and are involved in nociception, can be further subdivided into peptidergic and non-peptidergic classes. Despite the fact that there are several reports indicating a partial overlap among the markers *(Carr et al., 1990; Wang et al., 1994; Bergman et al., 1999; Kashiba et al., 2001)*, it is generally accepted that peptidergic neurons release calcitonin gene-related peptide (CGRP) and substance P (SP) as well in most of the cases, and they express the nerve growth factor (NGF) receptor TrkA. On the other hand cells in the non-peptidergic population bind the Griffonia Simplicifolia B4 isolectin (IB4), they express the fluoride-resistant acid phosphatase (FRAP) as well as a specific purinergic receptor subtype $P2X_3$ and they express the c-Ret neurotrophin receptor, which is responsive to the glial cell line-derived neurotrophic factor (GDNF) *(Nagy and Hunt, 198; Hunt and Rossi, 1985; Snider and McMahon, 1998; Silverman and Kruger, 1988; 1989; Julius and Basbaum, 2001; Willis and Coggeshall, 2004; Zeilhofer et al., 2012)*.

Central processes of the primary sensory neurons form the dorsal root of the spinal cord. Upon entering the cord, primary afferent fibers bifurcate into a rostral and a caudal branch, travelling in the dorsal coloumn in case of large diameter afferents and in the tract of Lissauer in case of fine caliber fibers, and give rise to several collaterals which enter the dorsal horn *(Davidoff, 1984)* to establish synaptic connections with secondary sensory neurons. Vast majority of the primary afferent synaptic input is accepted by interneurons, or so called local circuit neurons (LCNs), the axons of which remain in the spinal cord and arborize locally *(Todd, 2010)* to establish extensive synaptic connections with different neuronal populations of the spinal cord. As these synaptic connections originate from and terminate in the spinal

cord itself, they are mentioned as propriospinal. Although in the previous decades serious progress have been made in the research of the complex neuronal circuitry of the dorsal horn, our knowledge of its detailed function is still far from complete. However, these neuronal networks presumably perform the primary processing of the nociceptive input. Another key neuronal group in the dorsal horn circuitry is that of projection neurons, receiving synaptic input mostly from local interneurons, and in a lesser proportion directly by primary afferent fibers *(Pinto, 2010)*. Projection neurons provide connection from the dorsal horn to supraspinal centers via their long axons, which, after crossing the midline to the contralateral side (in most but not all cases), form the ascending nociceptive pathways. It was recently suggested that projection neurons can also contribute to local and propriospinal connections via their collateral axonal branches *(Szücs, 2010)*.

The nociceptive pathways ascend in the anterolateral quadrant of the spinal cord white matter and form a thick bundle of fibers, which is commonly referred to as the anterolateral system or anterolateral tract (ALT). Majority of the fibers is given by the anterior and lateral spinothalamic tract, which target various nuclei in the thalamus. The importance of the thalamic projections is possibly dual: while the lateral part of thalamus is thought to be involved in discriminative pain, the medial part of it is possibly related to the motivational aspects of pain *(Kenshalo, 1968)*. Besides the direct spinothalamic projections, two indirect pathways have to be mentioned, which provide polysynaptic connection between the spinal cord and the thalamus: the spino-cervico-thalamic pathway via the lateral cervical nucleus and the postsynaptic dorsal coloumn system, via the dorsal column nuclei *(Millan, 1998; McMahon and Koltzenburg, 2006)*. However, it has to be noted, that although in primates the thalamus is the predominant target of spinal cord projection neurons, in rodents most of the projection neurons terminate in the brainstem parabrachial nucleus *(Braz et al., 2014)*. Another important brainstem target of nociceptive pathways is the periaqueductal grey *(Bernard et al., 1995)*, which is involved in descending antinociceptive modulation via its projections to raphe magnus nucleus, catecholamine cell groups and the reticular formation. These spinobulbar projections in general are responsible for the integration of nociceptive activity with processes that subserve homeostasis and behavioural states. Besides the spinothalamic and spinobulbar projections, retrograde labelling experiments indicate the presence of a spinohypothalamic pathway *(Burstein et al., 1990)*, which can have a potential role in

the autonomic, neuroendocrine and emotional aspects of pain *(McMahon and Koltzenburg, 2006)*.

Projections from the thalamus, hypothalamus and the brainstem provide multiple inputs to various forebrain regions. Therefore the final complex experience of the sensation of pain cannot be linked to one distinct cortical region *(Apkarin et al., 2005)*, instead, it is a result of the activation of various cortical sites, including the sensorimotor cortex at the central sulcus, the parieto-insular region near the operculum, the anterior insula and the anterior cingulate *(McMahon and Koltzenburg, 2006; Craig, 2003).*

Cellular and molecular anatomy of the spinal dorsal horn

The grey matter of the spinal cord can be grossly divided to a ventral horn, location for neurons involved in motor functions and to a dorsal horn, which is responsible for sensory functions. Based on cytoarchitectonic features, the grey matter can be further subdivided into ten laminae *(Rexed, 1952),* out of which laminae I (marginal layer), II (susbstantia gelatinosa), III and IV (nucleus proprius), V and VI comprise the dorsal horn *(Millan, 1998)*. Lamina I and the outer two-third of lamina II (lamina IIo) is often mentioned as superficial dorsal horn in literature *(Basbaum and Bushnell, 2009),* and bears special importance in the processing of painful stimuli, as it is densely innervated by nociceptive fibers, while low threshold mechanoceptor input is lacking from this area *(Zeilhofer, 2012).* Cutaneous nociceptive Aδ fibers project predominantly to lamina I, but to a lesser extent they also provide input to lamina IIo, while peptidergic C fibers terminate primarily in lamina IIo, and non-peptidergic C fibers target mostly lamina IIi, Besides the superficial dorsal horn, it is lamina V, VI and X, which contribute to the reception, processing and rostral transmission of nociceptive information *(Millan, 1998)*.

Neurons of the dorsal horn can be classified according to several aspects. Regarding their response to nociceptive input, one can distinguish nociceptive specific (NS) neurons, which are exclusively activated by unmyelinated C and thinly myelinated Aδ primary afferent fibers carrying high threshold noxious stimuli *(Millan, 1998)*. These neurons, not responding to innocuous stimuli in normal conditions, occur in highest density in lamina I and IIo, whilst in a lesser amount they

can also be found in lamina V and VI. The second group of neurons is the multireceptorial or wide-dynamic range (WDR) neuron *(Millan, 1998)*, which encodes input intensity by producing a dynamic response over a broad range of stimulus strength *(Dubner et al., 1989)*. Another specificity of these neurons is that they display massive convergence from cutaneous, muscle and visceral input *(Mense, 1993; Ness and Gebhart, 1990)* and they can be excited by thermal, mechanical and chemical stimuli carried by C, Aδ and also Aβ afferent fibers. WDR neurons are mainly located in lamina V, but they can also be found in lamina IV and VI, and in a lesser amount in lamina I, IIo and X as well. The third group of dorsal horn neurons is non-nociceptive (NON-N) - these neurons are mostly found in lamina II, III and IV *(Millan, 1998)*.

Although most authors agree that the majority of lamina I neurons respond to noxious stimulation, their exact proportion compared to neurons responsive to other input modalities is not clarified and the rate of nociceptive specific and wide dynamic range neurons is likewise unclear. Light *(Light, 1992)* reports that 63% of lamina I neurons are nociceptive (28% responsive only to noxious mechanical, while 35% responsive to noxious mechanical, noxious heat and chemical stimuli), 12% are innocuous thermoreceptive neurons, 14% respond to innocuous mechanical stimuli and 5% respond to both innocuous mechanical and noxious stimuli. According to Andrew and Craig *(Andrew and Craig, 2002)* 61% of spinothalamic neurons originating from lamina I are nociceptive, of which 43% was defined as nociceptive specific and 57% proved to be wide-dynamic range neuron, while 39% of lamina I neurons projecting to the thalamus are responsive to innocuous thermal stimulation. In lamina II, while the inner part is containing innocuous mechanically responsive neurons, the outer two-third is considered to comprise in a great proportion of nociceptive neurons. According to different publications *(Light et al., 1979; Light and Kavookijan, 1988; Light and Willcockson, 1999)*, around 70% of lamina IIo neurons are nociceptive, 5% of them respond to innocuous thermal and another 5% to innocuous mechanical stimuli, while 20% is responsive to both nociceptive and innocuous mechanical stimuli *(Basbaum and Bushnell, 2009)*.

Dorsal horn neurons can also be classified according to their output destination *(Willis and Coggeshall, 2004)*. Projection neurons, which target supraspinal centres, can be found in highest density in lamina I, while they are only scattered from lamina III to VI and very sparse in lamina II *(Todd, 2010)*. Though, it

has to be noted, that even in lamina I, where the presence of projection neurons is estimated the highest, they presumably don't make up more than five to nine per cent of all neurons *(Spike et al., 2003)*. Although not entirely specific *(Al Ghamdi et al., 2009)*, around 80% of lamina I projection neurons express the neurokinin 1 (NK1) receptor, which is activated by substance P *(Marshall et al., 1996; Todd et al., 2002).* It has to be noted, that recently lamina I local-circuit neurons were also shown to express functional NK1 receptors *(Luz et al., 2014).* Projection neurons of the dorsal horn receive input from segmental interneurons *(Dahlhaus et al., 2005; Polgar et al., 2008; Puskar et al., 2001; Luz et al. 2010)*, descending antinociceptive pathways *(Polgar et al., 2002)* and can also be directly excited by C and Aδ primary afferents *(Pinto et al., 2010; Luz et al., 2014; Dahlhaus et al., 2005; Ikeda et al., 2003)*. It is noteworthy, that as lamina I projection neurons don't receive innocuous input, they are regarded as nociceptive specific *(Zeilhofer, 2012)*. While projection neurons obviously play an important role in the supraspinal transfer of nociceptive information, at the same time, they can be involved in the establishment of propriospinal connections by giving rise to numerous local collaterals along their route in the spinal cord *(Szücs et al., 2010)*.

On the other hand, vast majority of dorsal horn neurons remain in the spinal cord to arborize locally, and can be defined as interneurons. This latter is a largely heterogeneous group, including virtually all of lamina II neurons, and representing the majority of neurons in lamina I and III. Interneurons are directly activated by C and Aδ primary afferent fibers, and in addition they can be activated by descending antinociceptive pathways *(Millan, 2002)*. Unlike projection neurons, which can only be excitatory *(Littlewood et al., 1995)*, interneurons can be either excitatory, or inhibitory, moreover some of them can exert both actions *(Millan, 1998)*, and they also represent high variability in their neurohistochemical profile. Excitatory amino acids play a putative role in mediating the excitatory actions of interneurons *(Millan, 1998)*, furthermore many neuropeptides, like substance P, neurotensin or VIP, which have been revealed in these neurons, may be involved as well *(Dubner and Ruda, 1992; Todd and Spike, 1993; Todd et al., 1994)*. Inhibitory interneurons use gamma-aminobutyric acid (GABA) as primary neurotransmitter, but around half of them are also immunoreactive for glycine *(Todd and Sullivan, 1990; Spike et al., 1993; Todd and Spike, 1993),* although co-release of GABA and glycine from the same presynaptic vesicle does not necessarily mean that both transmitters contribute to

postsynaptic inhibition *(Zeilhofer, 2012)*. Besides glycine, 65% of GABAergic interneurons in lamina I and 50% of them in lamina II co-localize with neuropeptide Y (NPY), galanin (GAL), parvalbumin (PV) or neural nitric oxyd synthase (nNOS), and as these groups don't overlap, they define distinct subpopulations of inhibitory interneurons *(Braz et al., 2014)*. On the basis of the expanse of their axon cloud and propriospinal connectivity, interneurons can be intersegmental, interlaminar intrasegmental and intralaminar intrasegmental, also known as local, interneurons *(Millan, 1998)*. Although interneurons obviously play an important role in the inter- and intralaminar transfer, integration and modulation of nociceptive input *(Millan, 1998)* our knowledge about their proper axonal projections is still incomplete and the lack of this information constitutes a serious obstacle in the understanding of the operation of the dorsal horn neuronal circuitries *(Todd, 2010)*.

Neurons of the superficial dorsal horn can also be characterized on a morphological basis. Lamina II interneurons have been studied extensively from this aspect, and the results of patch clamp studies have greatly contributed to our present knowledge. According to the most widely accepted classification, which is based on dendritic morphology *(Grudt and Perl, 2002),* one can distinguish islet, central, vertical and radial cells. While islet cells are GABAergic *(Todd and McKenzie, 1989)* and are probably the main inhibitory neurons of the dorsal horn *(Braz et al., 2014)*, radial cells can be either inhibitory or excitatory *(Maxwell et al., 2007; Yasaka et al., 2010)* while central and vertical cells are predominantly excitatory.

Regarding lamina I, there are several classifications in the literature, Gobel describes two types of lamina I neurons, pyramidal with and without dendritic spines and multipolar with loose and compact dendritic arbor *(Gobel, 1978)*. Zhang and colleagues distinguish a third group of neurons, fusiform, besides pyramidal and multipolar *(Zhang et al., 1996; Zhang and Craig, 1997),* while according to the most widely accepted description of Lima and Coimbra, lamina I neurons belong to four groups: flattened, characterized by a flattened soma and a dendritic tree confined to lamina I; fusiform, with a longitudinal, spindle-shaped soma and numerous dendritic spines; pyramidal, with an elongated perikarya bulging into the white matter and multipolar with a dense dendritic arbor *(Lima and Coimbra, 1983; 1986)*. Although these morphological descriptions are hard to comply with functional features, Han and colleagues report that fusiform neurons are nociceptive, pyramidals are thermoreceptive, and multipolars are either polymodal or nociceptive *(Han et al.*

1998). At the same time, Todd reveals that NK1 receptors are expressed by fusiform and multipolar neurons, therefore these latter two may be regarded as nociceptive *(Todd et al., 2002).* As these classic morphological descriptions of lamina I neurons are based on the results of Golgi silver impregnation method, which doesn't stain the myelinated axon, they only take into account the somatodendritic architecture therefore they can't distinguish projection neurons from interneurons with high degree of certainty, which would be important regarding the functional consequences. Furthermore, knowing the proper axonal trajectory and detailed branching pattern of projection neurons and interneurons would bring us closer to reveal putative propriospinal connections and to better understand the operation of neuronal circuits of the dorsal horn. Szücs and colleagues recently managed to describe distinct morphological groups of projection neurons falling into the flattened, pyramidal or fusiform types of Lima and Coimbra in the lateral half of lamina I on the basis of their collateral branching pattern by combining intracellular labelling of individual neurons and three-dimensional Neurolucida-assisted reconstruction techniques. The main axon of the projection neurons they examined gave various ipsilateral collateral branches, crossed the midline in the anterior commissure in all cases and ascended in the contrelateral ALT. Szücs and collegues describe four neuronal groups with distinct collaterals 1) along the dorsal grey matter (dorsal collateral type, DCT), 2) parallel with the lateral edge of the dorsal grey matter, running rostrally or caudally (lateral collateral type, LCT), 3) in the ipsilateral ventral horn (ventral collateral type, VCT), and 4) projection neurons which give rise to more than one type of collaterals (mixed collateral type, MCT) *(Szücs et al., 2010)*. The authors conclude that DCT type projection neurons may play a role in the establishment of intrasegmental intra- and interlaminar connections, VCT neurons possibly target deeper (V-VIII) laminae and contribute to the dorsoventral sensory information flow in the dorsal horn, suggested by Braz and Basbaum *(Braz and Basbaum, 2009)* and the elongated lateral collaterals of LCT neurons may be involved in multisegmental integration of sensory information. On the other hand, projection neurons in the lateralmost part of lamina I and the neighbouring lateral spinal nucleus (LSN) have not yet been studied. Furthermore, we have almost no morphological description of the somatodendritic and axonal structure of lamina I interneurons.

The lateral spinal nucleus

The LSN, also known as the nucleus of the dorsolateral funiculus, was first described by Gwyn and Waldron. It consists of neurons scattered among the fibres of the dorsolateral funiculus (DLF), and unlike the lateral cervical nucleus, it forms a continuous column ventrolateral to the dorsal horn of the spinal cord from the spinomedullary junction to the sacral levels. Although it is present in rat, guinea-pig and ferret, it proved to be missing from human *(Gwyn and Waldron, 1968; 1969)*. The loosely organized nucleus differs from the dorsal horn in respect to the structure of its neuropil, as it is built up by myelinated and unmyelinated axons and neuronal cell bodies covered by boutons *(Olave and Maxwell, 2004).*

Neurons of the LSN can be labelled by retrograde axoplasmic transport techniques from various supraspinal loci, including the parabrachial nucleus *(Ding et al., 1995; Feil and Herbert, 1995*), the periaqueductal grey *(Pechura and Liu, 1986; Harmann et al., 1988)* the nucleus of the solitary tract (*Menetrey and Basbaum, 1987; Esteves et al., 1993)*, the medullary reticular formation *(Leah et al., 1988; Pechura and Liu, 1986),* the nucleus accumbens, the septum *(Burstein and Giesler, 1989)* and the amygdala and orbital cortex *(Burstein and Potrebic, 1993),* most of which are involved in sensory functions and some of them specifically in nociception. The diencephalic targets of LSN neurons include the hypothalamus *(Burstein et al., 1990)* and the thalamus *(Battaglia and Rustioni, 1992; Li et al., 1996; Marshall et al., 1996*). In contrast to the superficial dorsal horn, LSN projects bilaterally to the mediodorsal thalamic nucleus and some authors assume that this LSN-mediodorsal pathway may be involved in the emotional and cognitive aspects of pain *(Gauriau and Bernard, 2004)*. These results imply that the majority of LSN neurons are projection neurons, and this view is also supported by Réthelyi, whose morphological descriptions indicate that the axons of LSN neurons become myelinated soon after their origin *(Réthelyi, 2003)*, which is a common feature of projection axons. Besides supraspinal targets, LSN neurons also project to lamina I, II, V and VII of the spinal cord *(Jansen and Loewy, 1997)*. Réthelyi also mentions that LSN neurons could be double labelled from two injection sites in the brainstem and diencephalon, as well as in the brainstem and spinal cord *(Réthelyi, 2003)*, which raises the possibility that these neurons probably take part in the establishment of propriospinal connections via collateral axon branches.

In spite of its involvement in various nociceptive pathways, there are controversial experimental data about the primary afferent input to LSN. Electrophysiological experiments indicate that neurons of the LSN cannot be directly activated by cutaneous stimulation *(Giesler et al., 1979; Menetrey et al., 1980)* but some of them respond to movements of joints and deep tissue *(Menetrey et al., 1980),* at the same time visceral primary afferent input to the LSN cannot be excluded *(Sugiura et al., 1989)*. Immunohistochemical studies imply that LSN neurons don't receive input from myelinated, unmyelinated or peptidergic primary afferents *(Olave and Maxwell, 2004)*. Nonetheless, upon dorsal root stimulation most of the LSN neurons produce polysynaptic postsynaptic potentials *(Jiang et al., 1999),* while Pinto and colleagues report that LSN neurons receive monosynaptic projections from both Aδ and C fibers *(Pinto et al., 2010)*.

LSN neurons may receive majority of their synaptic input from spinal interneurons. Presence of considerable amount of peptidergic varicosities is said to be characteristic of the nucleus *(Olave and Maxwell, 2004)* and the number of peptidergic varicosities is not affected by dorsal rhizotomy or experimental lesions of the descending pathways, therefore several authors conclude that peptidergic input to LSN may arise from the same or nearby segmental levels of the spinal cord. *(Seybold and Elde, 1980; Cliffer et al., 1988; Giesler and Elde, 1985; Olave and Maxwell, 2004)*. On the other hand, occasional axon collaterals of lamina I projection neurons also enter the dorsolateral funiculus *(Grudt and Perl, 2002; Szücs et al., 2010)*, which can provide substrate for a putative synaptic connection to the neurons of the LSN, although such synaptic connections have not yet been demonstrated by electrophysiological methods.

It also has to be mentioned that besides primary afferent fibers and neurons of the dorsal horn, LSN also receives descending projections from the brainstem reticular formation, the dorsal column nuclei, from the raphe nuclei and the periaqueductal grey *(Carlton et al., 1985; Masson et al., 1991)*.

In contrast to the superficial dorsal horn, our knowledge of the LSN neuron morphology is far from complete. Based on the results of Golgi silver impregnation experiments, Réthelyi reports that although some spindle shaped neurons are present, the dominant morphological type of LSN neurons is multipolar *(Réthelyi, 2003)*. This finding is in accordance with previous results from intracellular labelling of LSN neurons *(Jiang et al., 1999)* and metabotropic glutamate receptor immunostaining

(Alvarez et al., 2000). The dendritic arbor of LSN neurons shows three preferential orientaion: in some cases the dendrites remained within the territory of LSN, while in other cases it was either directed laterally, or oriented medially in the direction of the dorsal horn *(Réthelyi, 2003)*. Laterally oriented dendrites often reached the surface of the spinal cord as it was already described by Bresnahan and colleagues *(Bresnahan et al., 1984),* which raises the possibility that LSN neurons can be directly affected by components of the cerebrospinal fluid. The medially oriented dendritic trees were described to overlap with the dendritic arbor of "neck cells", neurons by the edge of the grey matter, located at the junction of the dorsal horn and the intermediate zone, therefore the two parallel cell coloumns and the overlapping dendritic branches formed a ladder-like structure. This morphological similarity suggests a close relationship between the two neuronal groups *(Bresnahan et al., 1984)* and Réthelyi raises the possibility that LSN neurons are "neck cells" displaced into the grey matter *(Réthelyi, 2003)*. This idea is also supported by the similar electrophysiological features of LSN and deep dorsal horn neurons reported by Jiang and colleagues *(Jiang et al., 1999).*

It is noteworthy that despite the fact that most of the LSN neurons are supposed to be projection neurons, we don't know anything about their axon trajectories in the spinal cord, although it is possible that they take part in the establishment of propriospinal connections via collateral branches.

Despite the growing experimental data, little is known about the function of LSN. Immunohistochemical studies revealed that LSN neurons express NK1 receptors *(Brown et al., 1995; Littlewood et al., 1995; Ding et al., 1995; Marshall et al., 1996),* and there is a large array of peptides, which have been demonstrated in LSN neurons: vasoactive intestinal peptide (VIP), bombesin, dynorphin, calcitonin gene-related peptide (CGRP) *(Hökfelt et al., 1977; Nahin, 1987; Leah et al., 1988; Conrath et al., 1989; Battaglia and Rustioni, 1992)* and a significant amount of substance P (SP) (*Leah et al., 1988)*. LSN neurons were found to show immunoreactivity for the immediate early gene c-Fos in response to noxious thermal stimulation and unlike in case of the superficial dorsal horn, this immunoreactivity proved to be bilateral *(Olave and Maxwell, 2004).* These data together suggest that LSN may be involved in the processing of sensory stimuli, including nociception. As LSN neurons are more responsive to the electric stimulation of primary afferents than to natural cutaneous stimulation, the role of LSN may bear special importance in

pathologic conditions, such as hyperalgesia *(Jiang et al., 1999)*. Regarding its role in nociceptive information processing, LSN may function as an integrative nucleus, where neurons can receive inputs from primary afferents of visceral origin, interneurons and projection neurons of the spinal dorsal horn, descending pathways from supraspinal loci and can be directly affected by the components of the cerebrospinal fluid *(Olave and Maxwell, 2004)*.

Segmental and intersegmental propriospinal neural networks

It is widely accepted that the nociceptive information conveyed by primary afferent fibers is processed, modulated and integrated by neuronal networks of the superficial dorsal horn before transmitted to supraspinal centers. Our knowledge about the proper function of these networks is yet far from complete, although understanding their role in nociception would be strategically important in developing new analgesics. In the past decades several authors have reported numerous hypothetical network models, which tried to interpret the operation of neuronal circuitry in the superficial dorsal horn and its role in the modulation of nociceptive information. One of the oldest and probably the most acknowledged theory is the gate control theory, proposed by Melzack and Wall in 1965 *(Melzack and Wall, 1965)*. The model assumes that the nociceptive output signal from the spinal cord to the brain is determined by the balance of the activity of small diameter (nociceptive) and large diameter (non-nociceptive) primary afferent fibers which either open or close the gate, which symbolizes inhibitory interneurons in the superficial dorsal horn. As small diameter fibers not only activate projection neurons, but at the same time inhibit the inhibitory interneurons of the superficial dorsal horn, therefore open the symbolic gate in front of the nociceptive information flow. On the other hand, large diameter fibers activate the above-mentioned inhibitory neuronal network, which in turn inhibits projection neurons, therefore the hypothetic gate is closed.

While the main idea behind the gate control theory is still actual, by today numerous articles have been published revealing the enormous morphological and neurochemical heterogeneity of interneurons in the superficial dorsal horn, and researchers are attempting to map their connectivity and relation to each other. Based

on the results of paired electrophysiological recordings, Lu and Perl suggest that the superficial dorsal horn is organized into neuronal modules, in which specific neuron types establish highly selective connections with each other *(Lu and Perl, 2003; 2005)*. According to their observations, central cells of the inner part of lamina II, which receive monosynaptic input from C fibers, establish monosynaptic excitatory connections with vertical neurons of the outer lamina II, which receive monosynaptic input from C and Aδ fibers. As vertical neurons excite lamina I projection and non-projection cells, this pathway provides a ventral to dorsal excitatory drive to lamina I *(Braz et al., 2014),* which is in line with the results of Santos and colleagues *(Santos et al., 2007)*, who emphasize that sensory processing in the dorsal horn is dominated by excitatory connections, and those of Kato and colleagues *(Kato et al., 2009*), who report that the translaminar input pattern is greater in case of lamina I neurons and vertical cells than in cases of other neurons in the superficial dorsal horn. On the other hand a feedforward inhibitory control to lamina I is also apparent from the inhibition of vertical cells by islet cells *(Braz et al., 2014)*.

These models focusing mostly on the neuronal circuits involving lamina II neurons, presume that the nociceptive information processing is performed by local, segmental neuronal circuits in the superficial dorsal horn, which lack the connection to other parts of the spinal cord. However, there are more and more evidence supporting the original results of axon degeneration experiments*,* carried out by Szentágothai, who emphasized the importance of propriospinal neuronal networks *(Szentágothai, 1964)*. He reported that lamina II neurons establish short-range propriospinal connections via an intrinsic longitudinal unmyelinated axon system, which bridges distances of two to three mm. The existence of such connections have recently been reinforced by laser-scanning photostimulation experiments, carried out by Kato and colleagues *(Kato et al., 2009)*. More surprisingly, besides the short-range connections, Szentágothai also proposed a long-range propriospinal connection system via the lateral part of Lissauer's tract, which can bridge five to six spinal segments. Petkó and colleagues carried out axon tracing experiments *(Petkó and Antal, 2000; Petkó et al., 2004)* to investigate these putative propriospinal pathways and their results not only reinforce the existance of widespread propriospinal connectivity, but also draw the attention to substantial differences between the propriospinal connections of the medial and the lateral aspects of the superficial dorsal horn. They found that the lateral aspect bears much more widespread

propriospinal connections compared to the medial one. While a 300-400 μm–long section of the medial aspect sends and receives afferent fibers from a narrow cell column of the same territory which has a rostro-caudal extent of up to three segments, the propriospinal neurons of the same section in the lateral aspect project to and recieves input from a narrow cell column in the dorsal horn, which spreads all along the lumbar section of the spinal cord in the rostro-caudal extent. Petkó and colleagues also report that while the medial aspect projects powerfully in the direction of the lateral aspect, there are no fibers originating from the lateral part, which terminate in the medial part of the superficial dorsal horn. Petkó and collegues highlight that the lateral aspect of the superficial dorsal horn bears strong reciprocal commissural connections to the identical part of the contralateral superficial dorsal horn, which was not found in case of the medial aspect. They also ascertain that those fibers, which leave the dorsal horn in the direction of the ventral horn or to supraspinal centres originate almost exclusively from the lateral part of the superficial dorsal horn.

The widespread propriospinal connections of the lateral aspect of the superficial dorsal horn can at least partly originate from local collaterals of LCT projection neurons in lamina I, as suggested by Szücs and colleagues *(Szücs et al., 2010)*. On the other hand, a significant part of these long-range connections may originate from interneurons, but mainly due to technical reasons, there is no excessive morphological description and analysis available in literature of the extension and branching pattern of the axon cloud of these neurons. Besides the widely investigated superficial dorsal horn, it is tempting to assume that the LSN can be a potential target of these lateral long-range propriospinal connections, as Olave and Maxwell have already raised the possibility that LSN may function as an integrative nucleus in the processing of nociceptive sensory information *(Olave and Maxwell, 2004)*.

To further investigate the intersegmental propriospinal connections, paired electrophysiological recordings would be indispensable. Unfortunately, due to technical limitations of the generally accepted thin-slice preparations, up till recently, such experiments could have been carried out only in vivo with very low yield.

Oblique infrared LED illumination technique: a novel methodical approach in the in vitro electrophysiological research of propriospinal connections

Paired electrophysiological recording from adjacent neurons provides direct data of neuronal microcircuitries. The effectiveness of this technique can be highly increased if the selection and impalement of neurons is carried out under visual control. The traditional method for visualizing neurons in unstained preparations during patch-clamp recordings in *in vitro* conditions is differential interference contrast (DIC) microscopy, which uses transmitted light for the imaging, therefore besides cell cultures its application is restricted to thin-slice preparations *(Edwards et al., 1989)*. As the light passes through the specimen, a significant amount of scattering occurs, which depends on the thickness and optical densitiy of the preparation, and lowers the achievable resolution. Consequently, in case of slice preparations, the combination of electrophysiological recordings with DIC visualization technique is only applicable for some hundred-micrometer-thick slices and allows investigators to study only neuronal circuitries within these boundaries *(Safronov et al., 2007)*.

The oblique infrared LED (IR-LED) illumination technique provides imaging by using reflected light, which has much less scattering, therefore higher resolution can be obtained. Moreover, as the neurons are visualized in a reflected component of the light, the technique is not restricted to slice preparations and high quality images can be made from the cut surface of neuronal tissue blocks, regardless of their thickness and optical density *(Safronov et al., 2007)*. Szücs and colleagues reported that the IR-LED illumination technique can also be successfully applied to visualize neurons through the overlying white matter and introduced an unsliced, intact lumbar spinal block preparation, in which lamina I, II and occasionally lamina III neurons can be visualized through the fibers of the thin dorsolateral white matter in young rats *(Szücs et al., 2009)*. Using such spinal block preparation during patch clamp recordings makes it possible to intracellularly label intact neurons without truncating the dendritic tree, the widespread axon cloud of an interneuron or the ascending axon of a projection neuron *(Szücs et al., 2010)*. In addition it is also suitable for studying local microcircuits *(Luz et al., 2010)* and could be potentially applicable to investigate short and long range propriospinal connectivity.

The efficiency of investigating neuronal circuits can be further enhanced by using the cell-attached stimulation technique *(Santos et al., 2007)*, which allows testing an increased number of presynaptic neurons and putative neuronal connections compared to the conventional double patch clamp recording technique.

Combination of the oblique IR-LED illumination technique on intact spinal cord block preparation and cell-attached stimulation of putative presynaptic neurons provides a powerful tool for studying propriospinal neuronal networks.

Objectives

Our principal aim was to investigate the short and long range propriospinal connections in the lateral aspect of the superficial dorsal horn and analyse the neuronal participants by combined morphological and electrophysiological tools.

a) We aimed to provide an exhaustive morphological description of local circuit neurons and evaluate their putative contribution in propriospinal neuronal networks. In this aspect the axon bears special importance as it provides the output component of these neurons and knowing its expansion, target regions and trajectory would help us to assess their putative synaptic contacts.
b) We also wanted to investigate the latero-lateral segmental and intersegmental propriospinal connections, a significant number of which may be given by connections between lamina I and LSN neurons, by *in vitro* electrophysiological tools.
c) Finally, we wanted to take advantage of the possibility to label intact LSN neurons during the electrophysiological recordings to study their detailed morphology and axon trajectory. We also aimed to compare their characteristics of adjacent neurons in lamina I and place them in the existing knowledge of the dorsal horn neuronal circuitry.

MATERIALS AND METHODS

Spinal cord preparation

Young laboratory Wistar rats of age P14-P21 were decapitated after anesthesia by the intraperitoneal injection of Na^+-pentobarbital (30 mg/kg) and subsequent check for lack of pedal withdrawal reflexes.

The vertebral column was dissected and immersed in oxygenated artificial cerebrospinal fluid (ACSF) at room temperature. The spinal cord was accessed via laminectomy from the ventral surface. The ventral and dorsal roots were cut and the pia mater was removed with the help of a fine scissors and a forceps under a dissection microscope. The lumbar segment of the spinal cord was cut out and glued to a golden plate by cyanoacrilate adhesive with the dorsolateral surface facing up. The preparation was transferred to the recording chamber.

All animal study protocols were approved by the Animal Care and Protection Committees of the University of Debrecen and the Instituto Biologia Moleculear e Celular (IBMC).

Visualization and identification of neurons in lamina I and the LSN

Neurons were visualized by a Zeiss Axioskop FS microscope (Carl Zeiss Microscopy, USA) equipped with a X40 water immersion objective, custom made oblique infrared illumination and a CCD camera system (Hamamtsu, Japan)

Neurons in lamina I are accessible for tight seal recordings mostly lateral to the dorsal root entry point, as superficial neurons medial from here are hidden by the thick ascending and descending fibres of the dorsal funiculus in young rats *(Pinto et al., 2008b; 2010)*. The lateral aspect of lamina I was identified as a territory of grey matter, formed by cell bodies of around 20 μm surrounded by a network of randomly oriented fibres. The LSN was found ventrolateral to lamina I and identified as large neuronal cell bodies scattered among the parallel, rostrocaudally oriented fibers of the dorsolateral funiculus *(Figure 1.)*.

It has to be mentioned, that although the borderline between lamina I and the fibers of the dorsolateral funiculus is obviously visible on a two-dimensional image

(Figure 1.), in a three-dimensional preparation there is a slight overlap between the two regions, which forms a thin transitional zone. In some cases cell bodies in the above-mentioned transitional zone could be defined as lamina I or LSN neurons only after histochemical processing.

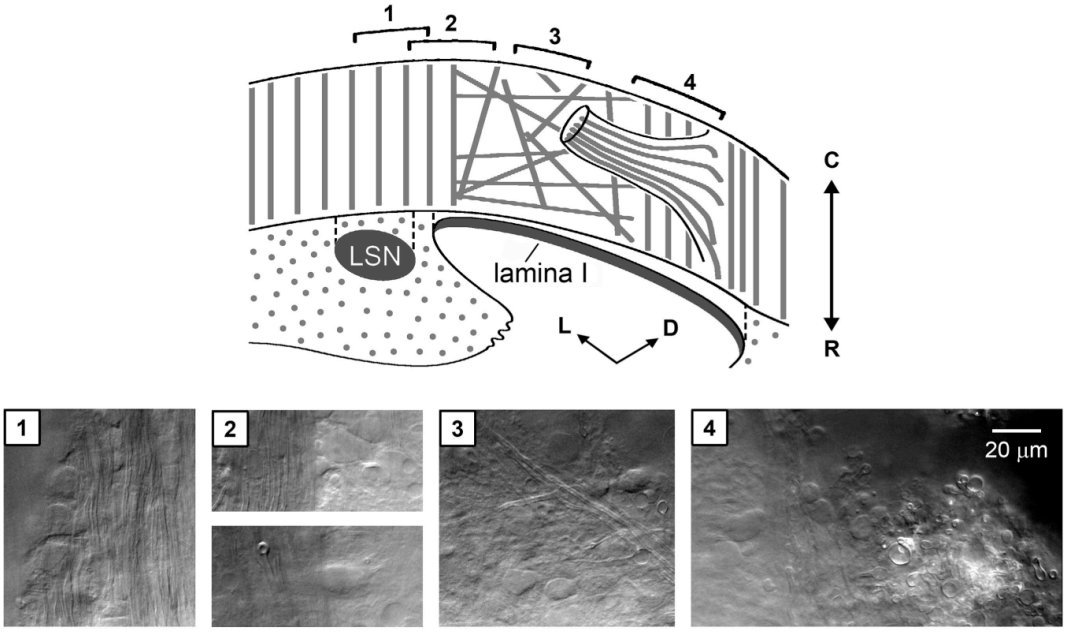

Figure 1. *Visualization and identification of lamina I and the LSN*
The schematic drawing demonstrates the orientation of fibers in the dorsal and dorsolateral funiculus (DF and DLF, respectively). The photomicrographs were taken from four representative areas indicated on the drawing. Area 1: LSN, large neuronal cell bodies scattered among thick parallel fibers of the DLF. Area 2: Transitional zone between the DLF (left) and lamina I (right). Area 3: Neurons in the lateral aspect of lamina I surrounded by a network of randomly oriented fibers. Area 4: The medial border of accessible part of lamina I (left) and myelinated fibers in the dorsal root entry zone (right). *Figure adapted from Pinto et al., 2010*

Electrophysiological recording and intracellular labelling of neurons

Patch-clamp recording of the postsynaptic neuron and intracellular labelling

Electrophysiological recordings from putative postsynaptic neurons in the lateralmost aspect of lamina I and the LSN were performed in whole-cell configuration. During the whole course of the experiment, oxygenated ACSF was perfused through the recording chamber, which was composed of: NaCl 115 mM,

KCl 3 mM, $CaCl_2$ 2 mM, $MgCl_2$ 1 mM, NaH_2PO_4 1 mM, $NaHCO_3$ 25 mM and glucose 11 mM (pH was 7.4 when bubbled with 95%-5% mixture of O_2-CO_2).

Pipettes were pulled from a thick-walled borosilicate capillaries (BioMedical instruments, Germany) by a vertical (Narishige PC-10, Japan) or a horizontal pipette puller (Sutter P-97, USA) and fire-polished afterwards (Narishige Microforge MF-830). The final resistance of the pipettes was ranging between 4-5 MΩ.

The pipettes were filled with an intracellular solution containing KCl 3 mM, potassium-gluconate 150 mM, $MgCl_2$ 1 mM, BAPTA 1 mM, Hepes 10 mM. The pH was adjusted by KOH to 7.3. The final [K^+] was 160 mM. Before the experiment biocytin (0.5-1%) was added to the intracellular solution with which the recording pipette was filled. To enhance the passive diffusion of bioctyin into the fine neuronal processes we applied repetitive depolarizing current pulses at the beginning and at the end of the recording session.

The experiments were carried out partly in the Instituto Biologia Molecular e Celular (IBMC, Rua do Campo Alegre 823, 4150-180 Porto, Portugal), where the amplifier used was EPC10-Double (Heka, Germany) and partly in the Department of Anatomy, Histology and Embryology (University of Debrecen, Nagyerdei krt. 98. 4032 Debrecen, Hungary), with an Axopatch 1D (Axon Instruments, USA) amplifier. The signal was low-pass filtered at 2.9 kHz and sampled at 10 kHz. Offset potentials were compensated before seal formation. Liquid junction potentials were calculated (15 mV) and corrected for using the compensation circuitry of the amplifier.

Stimulation and labelling of putative presynaptic neurons

We searched for putative presynaptic neurons in lamina I, one or two visual fields medially, and one to seven visual fields caudally from the recorded postsynaptic neuron *(Figure 2.)*. After establishing whole-cell configuration with the postsynaptic neuron, 2-3 landmark structures were noted at the caudal end of the view-field. Then, the objective of the microscope was moved caudally along the spinal cord until the landmarks disappeared at the rostral end of the view-field and putative presynaptic neurons were searched for in this region. The size of a single visual field under our conditions was approximately 180 μm. When measuring larger rostrocaudal distances, the above steps were performed repeatedly.

The stimulating pipette was filled with a solution containing 500 mM NaCl and 1.5% biocytin. The putative presynaptic cells were stimulated in cell-attached

configuration by a 1ms long current pulse of 100 nA, at a frequency of 1 Hz using an EPC10-Double (Heka, Germany) or an Axoclamp 2B (Axon Instrments, USA) amplifier.

At the same time we attempted to label the presynaptic neuron via the cell-attached pipette as described by Szücs and colleagues *(Szücs et al. 2009)* during the recordings. The diffusion of biocytin into the cell was facilitated by applying depolarizing current pulses of increasig amplitude (1-10 nA, 1 nA increment) at 1 Hz for 10 min.

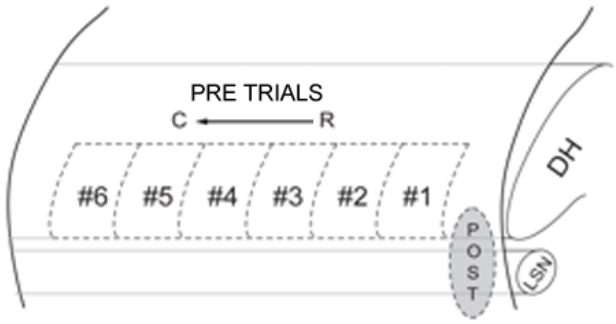

Figure 2. *Method of searching for putative presynaptic neurons*
The schematic drawing indicates the relation of the LSN to the dorsal horn (DH). The postsynaptic neuron, recorded in whole cell configuration, is located in the LSN or in the lateralmost aspect of lamina I (area indicated as „POST" on the drawing). The putative presynaptic neurons („PRE TRIALS") were tested in one or two visual fields medially and from one to seven visual fields caudally („C") from the recorded postsynaptic neuron.

Identification of monosynaptically connected neurons

Pairs of monosynaptically connected neurons were identified by using a protocol that contained a pre-pulse period (200 ms) followed by a single current pulse (100 nA, 1 ms) and a post-pulse recording period (200 ms) in which the postsynaptic neuron was recorded for 200 ms preceding and 200 ms following the current pulse application to the presynaptic neuron, and by analysing the stimulus-evoked changes in the excitatory postsynaptic current (EPSC) numbers. In some cases the pre-pulse recording was shorter (20 ms). The protocol was repeated 90 times at 1 Hz. EPSC latencies in connections were calculated from the end of the 1 ms stimulation pulse to the time moment when the evoked EPSC reached 10% of its peak amplitude. EPSCs in the pre-and post-pulse period were detected automatically by using MiniAnalysis (Synaptosoft, USA). Postsynaptic responses were considered monosynaptic if evoked EPSCs showed a low failure rate and a latency variation

below 4 ms. These criteria were based on a prior study in the intact spinal cord preparation *(Luz et al., 2010)* showing that lamina I neurons are directly connected by several parallel synapses via axodendritic pathways of different length, and therefore, latencies of individual components of a monosynaptic EPSC recorded in one connection can differ substantially. The monosynaptic nature of the connection was also verified by confirming the presence of transitions between individual EPSC components *(Santos et al., 2009; Luz et al., 2010)*. In case of those recordings, which were done with an Axopatch 1D amplifier (Molecular Devices, USA) the cell-attached stimulation of putative presynaptic neurons were carried out with an Axoclamp 2B amplifier (Molecular Devices, USA).

Histochemical processing

The preparations were fixed in 4% formaldehyde for at least 72 hours. After fixation the spinal cord was embedded in agar and 100 μm - thick sagittal sections were cut by a VT 1000S tissue slicer (Leica, Germany). To reveal biocytin, sections were permeabilized with 50% ethanol and treated according to the avidin-biotinyliated horseradish peroxidase (HRP) method (ExtrAvidin-Peroxidase, diluted 1:1,000; Sigma) followed by a diaminobenzidine (DAB) chromogen reaction. Sections were either counterstained on slides with 1% toloudine blue, dehydrated, cleared and coverslipped with DPX (Fluka, Switzerland) or treated with 1% OsO_4 and embedded in epoxy resin (Durcupan; Fluka, Switzerland). Phtotmicrographs were taken using the 10x or 40x dry lens of a Primo Star (Carl Zeiss Microscopy, USA) microscope equipped with a Guppy (Allied Vision Technologies, Germany) digital camera. Contrast and brightness of the photographic images used in all the figures were adjusted using the Adobe Photoshop software.

3-D reconstruction of labelled neurons and analysis

Complete 3-D reconstructions were done from serial sections using Neurolucida (MBF Bioscience, USA).

Each section was completely traced, using a X40 (dry) objective, onto the corresponding section of a serial section data set. In order to completely cover the

video image of the labelled process, we continuously adjusted the calibre of the digitally traced processes. The software, based on prior calibration, automatically set fibre calibre units for the selected lens. At any issue, we used a x100 (oil immersion) lens to determine Z differences of crossing structures.

We aligned the sections and connected the matching pieces working always in the direction of the section containing the soma. As a result of shrinkage during the histochemical processing the thickness (Z dimension) of resin-embedded sections was 80-90% of the original 100 μm. As this was comparable to the shrinkage along the X-Y axes, it was not corrected in these cases. In case of DPX-embedded sections, the shrinkage along the Z axis was corrected to reach the thickness of 80 μm and to be comparable to the other reconstructions.

Section contours, grey matter and central canal borders were traced at the bottom of each section.

Neuronal processes that could not be connected due to partial filling, distortion of the section or any other technical problems, were deleted from the data set. The percentage of such deleted processes is estimated less than 5%.

Morphometric analyses and basic quantitative measurements including Sholl analysis, dendritic segment length calculation, spine numbers, spine density and Fan-In projection were performed by Neuroexplorer (MBF Bioscience, USA). During the Fan-In projection a vertical axis is placed through the neuron. A virtual plane is swept around the axis collecting tracings of the dendritic structures. After sweeping through a full 360 degrees the plane has collected all of the dendritic structures that appear on the same side of the plane. The Fan-In projection was used to understand any preferred orientation in the dendritic processes. The Fan-In grid displays distance and angle. The processes are aligned so that all begin at the origin of the grid. Randomly oriented processes evenly cover the grid. Preferentially oriented processes trend more in some directions than other directions.

Calculation and 3-D visualization of varicosity distributions and action potential propagation time maps

In order to perform spatially dependent morphometric analysis on the axonal trees, we created a set of specific functions (called Py3DN; https://sourceforge.net/projects/py3dn/) in the Python programming language. The

Neurolucida data of the reconstructed axons were made available to the Python environment via a custom-made sparser. So that the spatially dependent results could be visualized, the morphometric analysis algorithms were integrated into Blender, which is a well-established, free, open source 3-D content creation site (www.blender.org).

For visual representation of the varicosity distribution along the axonal tree, we created a virtual boundary box that encompasses the entire axonal tree of the LCNs, which was then divided into 100 x 100 x 100 μm sized voxels. The number of the varicosities was calculated in each voxel, and we used its normalized value to color-code each voxel. The normalized value was also used to set the opacity index of the voxels, so that we could avoid problems of visualization in case of overlapping structures.

For creating propagation time maps along the LCN axonal tree, we calculated the time needed for a hypothetical action potential to reach each point of the axon, starting from the initial segment. We assumed that the contribution of each segment to the propagation time depends on its length and diameter. The equation used for calculating the propagation time δ of myelinated regions was $\delta = l/(kd)$ where l is length, k is a constant factor, which was equal to 10 m/second *(Cervero et al., 1979)* in case of myelinated and 380 m/second *(Pinto et al. 2008a)* in case of unmyelinated axonal segments, and d is the diameter. The diameter threshold we used to distinguish between myelinated an unmyelinated segments, was based on electron microscopic measurements. Finally we color-coded each point of the axon to represent the cumulative propagation time.

Calculation and 3-D visualization of varicosity distributions and action potential propagation time maps were performed by Paulo Aguiar (IBMC, Porto) and Péter Szücs

Electron microscopy

Those spinal cords, which were intended to be sent for electron microscopic analysis, were fixed in a mixture of 4% formaldehyde and 0.1% glutaraldehyde. After fixation, 100 μm-thick serial sagittal sections were made by a VT1000S tissue slicer (Leica, Germany), and the sections were permeabilized by freeze-thaw cycles in

liquid nitrogen. Biocytin was revealed according to the HRP-DAB protocol *(for details see chapter: Histochemical processing),* then sections were postfixed in 1% OsO_4, dehydrated, and embedded into epoxy resin (Durcupan; Fluka) on glass slides.

Regions of interest were excised and re-embedded for ultrathin sectioning. Ultrathin sections were further contrasted by lead citrate and uranyl acetate, and then scanned by a JEM 1400 TEM type electron microscope (JEOL, Japan). We recorded images of the biocytn-filled axonal profiles with the help of an SC 1000 Orius CCD camera (Gatan, USA) at x 20,000 or x 50,000 magnifications.

Electron microscopic images were taken by Péter Szücs with the help of Rui Fernandes (IBMC, Porto).

Statistical analysis

All statistical analyses were performed with the SigmaStat 3.0 (Systat Software, USA) software. Comparison of morphometric parameters between lamina I neurons and cells in the lateral adjacent white matter and LSN was done by using Student´s t-test or Mann-Whitney Rank Sum Test. Between-group comparisons of EPSC kinetic parameters were done by Kruskal-Wallis One Way Analysis of Variance on Ranks followed by Dunn´s Pairwise Multiple Comparison. A $p<0.05$ was considered to be statistically significant.

Numbers are given as mean ± SEM unless otherwise mentioned.

RESULTS

Morphology of local circuit neurons in lamina I

Our research group performed a thorough morphological description of lamina I LCNs, involving eighty-two neurons, out of which thirteen have been completely reconstructed in 3-D, which allowed us to accomplish further analysis.

The mean soma diameter of LCNs was 22.4 ± 0.6 μm (n=72) and the majority of the recovered neurons fell into the multipolar and flattened somatodendritic types of *Lima and Coimbra (1986)*. This is in line with earlier results of our group *(Szücs et al., 2010)* that none of the large multipolar neurons proved to be projection neurons. While the dendrites of flattened neurons were mostly restricted to lamina I and outer lamina II, some of the multipolar neurons possessed a dendritic arbor, which protruded ventrally and reached lamina III.

Extent of the axon

Although the axon of lamina I LCNs showed characteristic and distinguishing traits in some aspects, the lack of any axon in the contralateral white or grey matter and the presence of numerous ipsilateral, local axon collaterals with varicosities proved to be their common feature.

The axon of LCNs formed a local accumulation, which in most of the cases occupied the dorsal 100-120 μm thick band of the grey matter, corresponding the superficial dorsal horn and occasionally reached lamina III. While the mean mediolateral and dorsoventral extent of the labelled and recovered axon was 636 ± 27 μm and 295 ± 41 μm, respectively, the rostrocaudal spread was significantly higher, 2312 ± 116 μm, which corresponds to two to three lumbar spinal segments of rats at this age. The local network was either centred on the soma, or shifted along the rostrocaudal axis. In some cases, LCNs situated in the lateralmost part of lamina I had the majority of their axons located medially, several tens of micrometres away from the soma *(Figure 3)*.

Apart from the above-mentioned local axon, the majority of lamina I LCNs had single or multiple, varicose or myelinated-appearing, solitary axon branches in the neighbouring white matter, including the Lissauer tract, dorsal funiculus (DF),

dorsolateral funiculus (DLF), and lateral funiculus (LF). Some of these soliter branches gave rise to varicose unmyelinated collaterals of various density at certain distances form the main axon cloud. The presence of such remote targets (*e.g. in case of cell Zs022_E8-1 in Figure 4*) suggested us to perform further analysis of the fine structure and organization of LCN axons.

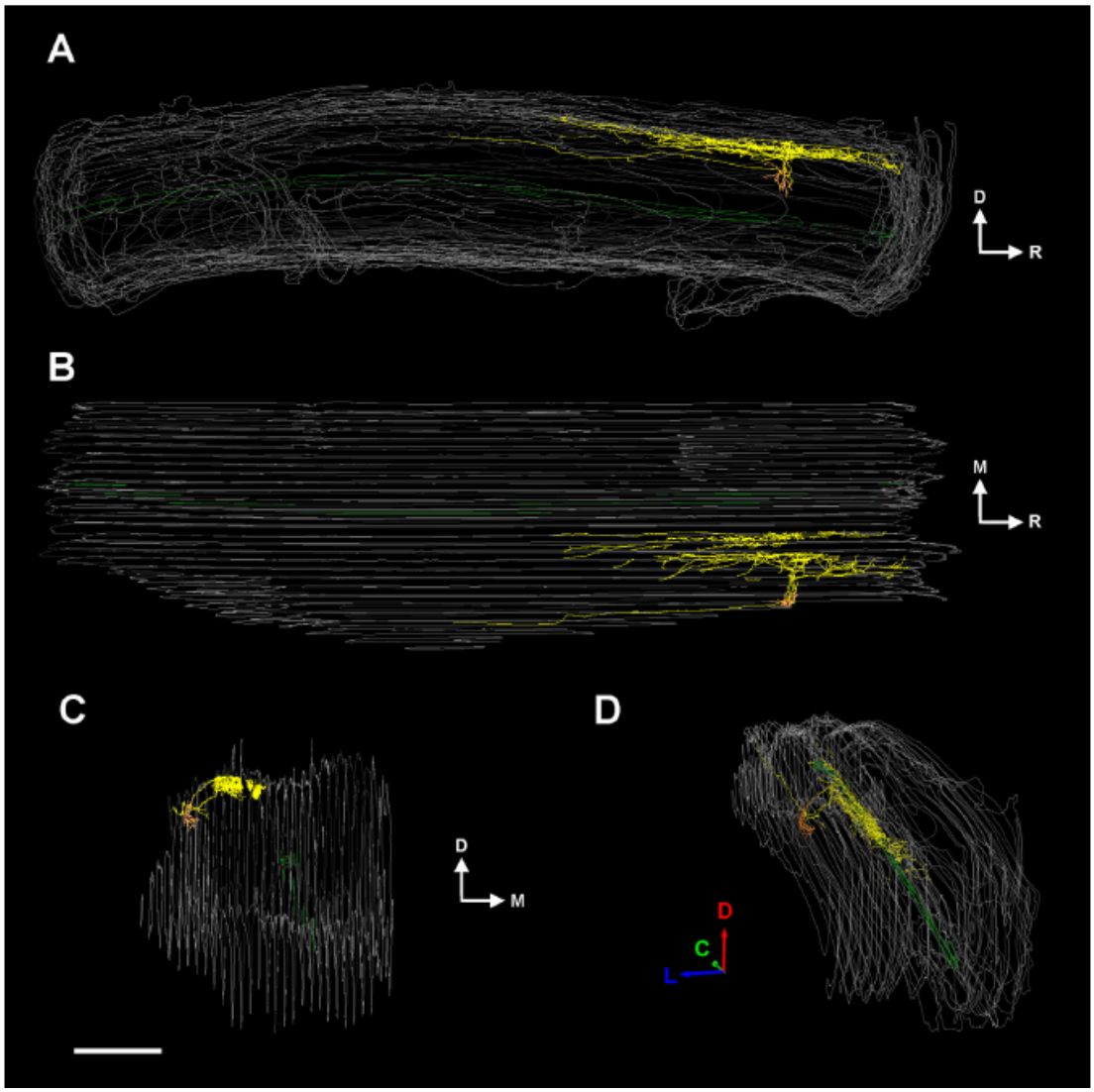

Figure 3. *Sagittal (**A**), horizontal (**B**), transverse (**C**), and perspective (**D**) view of a 3-D reconstructed but not fully connected LCN (cell ID: Zs079_E13)*
The majority of the axon (yellow) in this case is located medially, considerably remote from the lateral cell body and dendrites (orange). The neuron has a solitary branch running caudally in the dorsolateral funiculus on the ipsilateral side. The medial part of the axonal tree, because of distortion of some sections, could not be connected to form a single axon. White and grey matter borders are indicated with grey, and central canal is shown in green. Scale bar = 1 mm.

Branching pattern and varicosity distribution along LCN axons

By color-coding the primary axon branches of lamina I LCNs, we gained insight into their distinctive branching pattern. While some neurons of our sample possessed an axon, which only had three or four primary branches, and the proximal ones dominated the tree, in other cases the main axon gave rise to up to seven primary branches and the distal ones occupied more space. Regardless of the initial branching pattern, we found major or minor overlaps between target areas of the primary branches in all cases. The overlap ranged from slight *(Figure 4., Zs022_E8-1)* to substantial *(Figure 4., L395_E2)*.

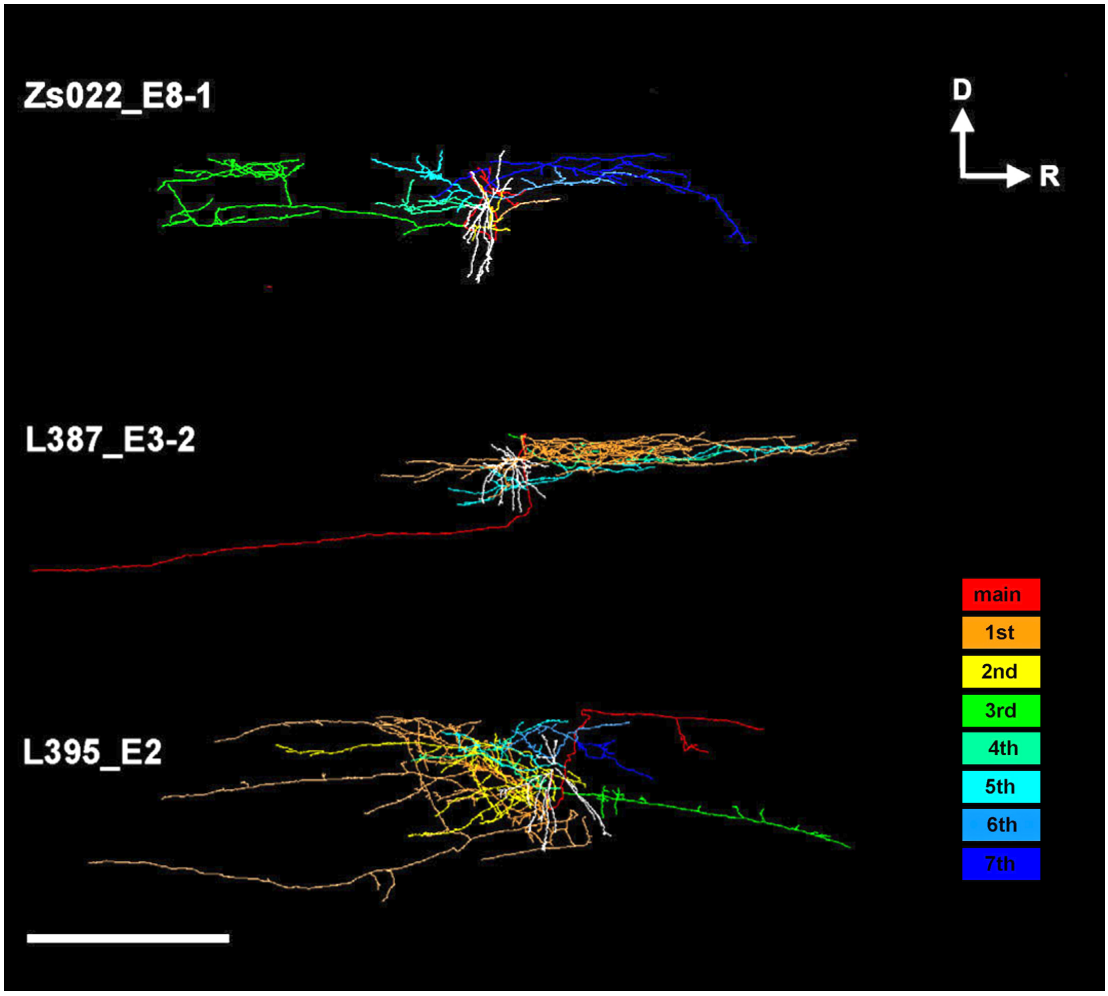

Figure 4. *Organization of primary axon branches of LCNs*
Sagittal view of 3-D reconstructions of three lamina I LCNs. In case of Zs022_E8-1 the tree is dominated by distal primary branches, and show limited overlap between the arbors. Two other neurons, L387_E3-2 and L395_E2, present axon trees dominated by primary branches that overlap substantially. Cell IDs are indicated on the left, next to the corresponding reconstruction. Colored boxes in the lower right corner indicate the color codes of the sequence of primary axon branches. S/d, soma and dendrites; main, main axon; 1st-7th, order of primary branches from the main axon. Scale bar = 1 mm *Author's contribution: acquisition of data, 30% contribution.*

Mapping of varicosity density along the axon combined with path distance measurements and Sholl analysis revealed characteristic patterns of varicosity distribution in case of lamina I LCNs. As a general feature, neurons presented the highest number of varicosities in the vicinity (within the first 500 μm) of, but not centred on, the soma. In some cases the number and density of varicosities gradually decreased farther from the soma *(Figure 5., L395_E2, L387_E3-2).* On the other hand there were cells in our sample, which presented fewer varicosities in the first 500 μm, but further local accumulations could be observed occasionally several hundreds of micrometers away from the soma in the rostrocaudal *(Figure 5., Zs022_E8-1)* or in the mediolateral axis. In these cases path distance histograms showed a more widespread distribution, compared to the previous group, with multiple peaks.

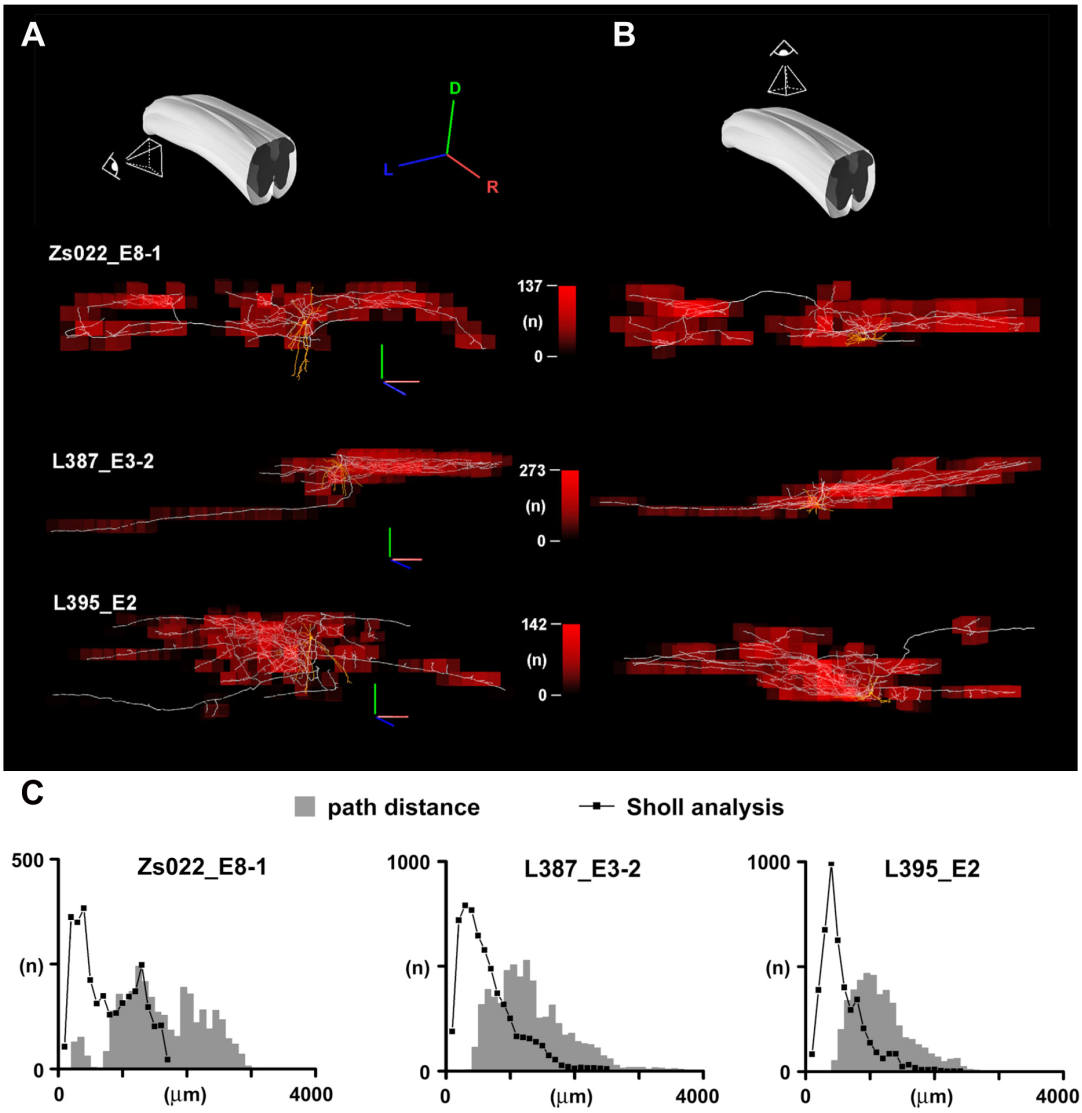

Figure 5. *Varicosity distribution along axons of LCNs*

Spatially dependent visual representation of axon varicosity distribution from sagittal (**A**) and horizontal (**B**) views, as indicated on the schematic drawings above each column. Axon varicosities along the 3-D reconstructed LCN axons were counted in predetermined space units (voxels). The maximum varicosity number in the predefined voxels (100 µm X 100 µm X 100 µm) is indicated as the maximum value (red) on the scale bar next to the particular neuron. The actual number of varicosities in a voxel is used as a color and opacity value for the cube representing that voxel. Cell IDs are indicated at left. 3-D scale bars (D, dorsal, green; L, lateral, blue; R, rostral, red) = 250 mm. **C:** Physical and path distance of axon varicosities in 3-D reconstructed LCN axons. Zs022_E8-1 with a lower overall number of varicosities, showing aditional accumulations, evidenced by multiple peaks in the Sholl analysis, and at the same time wider distribution of the path distance histogram. L387_E3-2 and L395_E2 showing a major accumulation of varicosities in the vicinity of, but not centered on, the soma, with one peak both in the Sholl analysis and in the path distance histogram. *Author's contribution: acquisition of data, 30% contribution.*

Fine structure of LCN axons and their effect on propagation time maps

The observation that sometimes remotely located varicosity bearing thin axon pieces were branching from myelinated appearing thicker axons raised the possibility of a presumable ultrastructural difference between the morphologically different parts. In order to clarify this matter our research group performed electron microscopic analysis of a characteristic section, where both types of axon were present *(Figure 6. A-B)*. We found that axonal profiles from the part of the section shown in *Figure 6. C-D* presented several concentric layers of myelin without exception, and diameter measurements showed that these parts were 760 ± 28 nm (n=24) with, and 453 ± 18 nm thick without myelin sheath (*Figure 6. G-I*). On the other hand, axon profiles from a varicose axon region (*Figure 6. E-F*) lacked myelin in case of both varicosities and intervaricosity segments, and the mean diameter of these unmyelinated parts was 311 ± 10 nm (n=157, *Figure 6. J-L*).

To determine how the different axon segments contribute to action potential conduction in the LCN axons we used a custom-made script, written in the Python programming language to create propagation time maps, in which we color-coded the propagation time values for all points of the 3-D reconstructed LCN axons. Based on the means and histograms of the measured diameters (*see Figure 6. I and L*), we determined a threshold (0.35 μm), above which the axon segment was considered myelinated. Conduction velocity in the unmyelinated part was set to 0.38 m/s for a uniform 1 μm thick axon *(Pinto et al., 2008),* and to 10 m/s in case of myelinated axons *(Cervero et al., 1979)*. When propagation time maps were calculated considering axon segments with a diameter above 0.35 μm as myelinated, the maximum propagation times dropped compared to those values, which were calculated by considering all axons unmyelinated. This change was negligible in case of the LCN with a compact tree, lacking remote regions attached via thick, long solitary branches (*not shown in the thesis, see Figure 10 in Szücs et al., 2013*). However, in case of LCNs with a remotely situated terminal branching area the maximum propagation time dropped to about 80% of the original value *(Figure 7.)*.

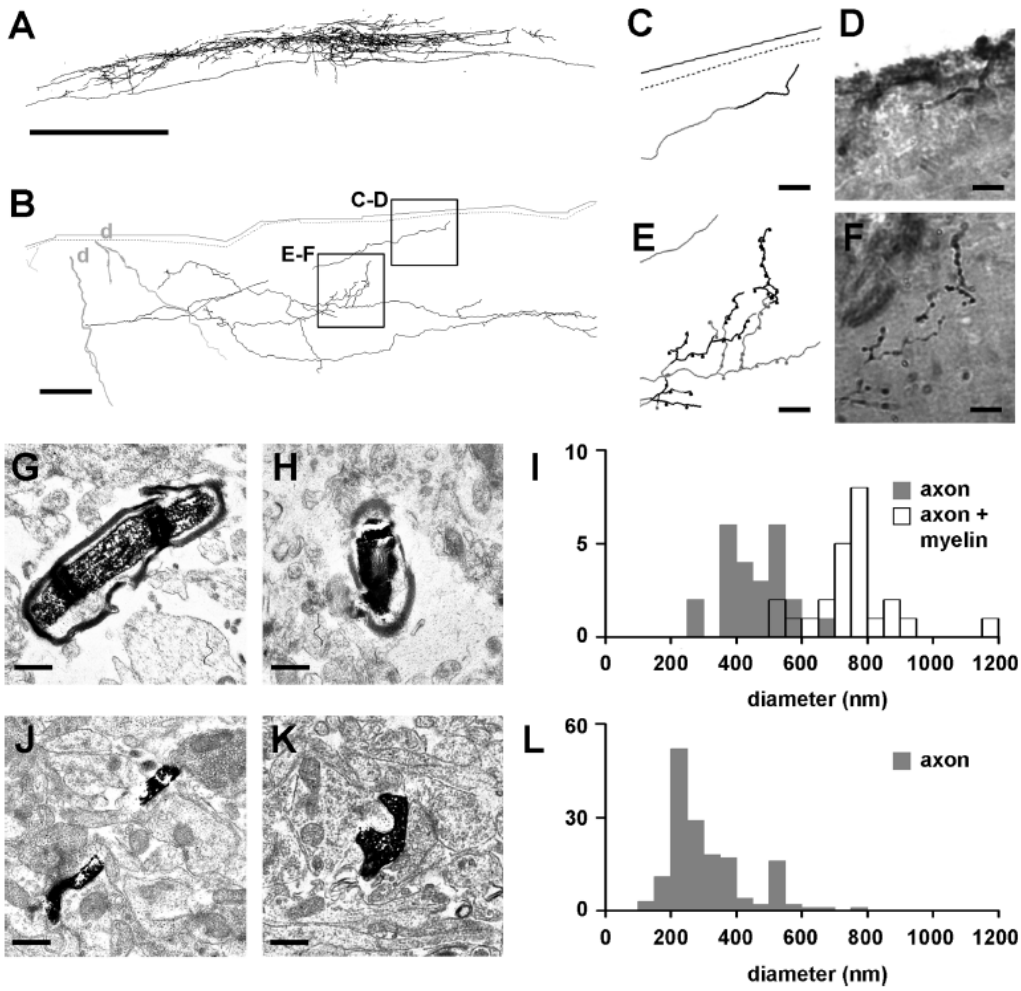

Figure 6. *Fine-structural difference between myelinated and unmyelinated parts of an LCN axon*

A: 2-D reconstruction of a representative LCN axon (cell ID: L279_E2). **B**: 2-D reconstruction of a single section of the same axon. Light grey processes are dendrites (d); the axon is in black. Continuous and dotted grey lines indicate the border of the section and border between the grey and white matter, respectively. Boxes indicate regions of interest with a single myelinated-appearing axon branch (C,D) and several varicose branches (E,F). **C–F** show the reconstruction of the corresponding region and a photomicrograph of the same region from the surface of the block used for preparing the electron microscopic sections. Black parts of the reconstructions in C,E show axon pieces still present on the block surface, whereas grey indicates parts that were already cut. **G,H**: Electron microscopic images of axon profiles from region C,D with several concentric layers of myelin. **I**: Diameter histogram of axon profiles (n . 24) from the same region measured with (open bars) and without myelin (shaded bars). **J**: Electron microscopic image of an intervaricosity segment and a varicosity (**K**) from region E,F. **L**: Diameter histogram of axon profiles (n . 157) from the same region. Bins . 50 nm in I,L. Scale bars . 1 mm in A; 50 μm in B; 10 μm in C–F; 500 nm in G,H,J,K. *Electron microscopic images were taken by Péter Szücs and Rui Fernandes.*

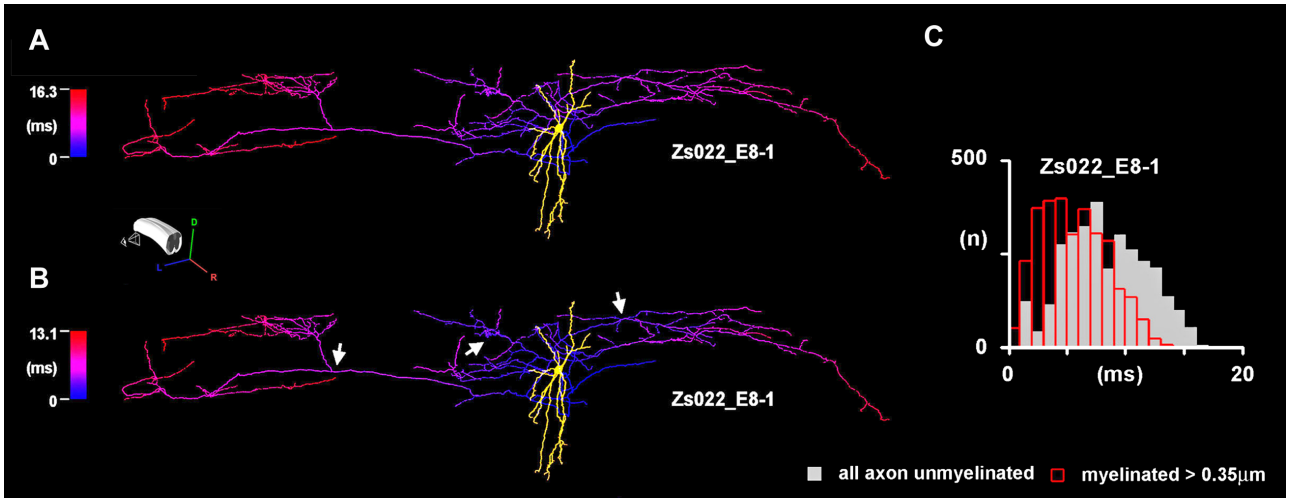

Figure 7. *Action potential (AP) propagation time maps of LCN axons*
A: Sagittal view of an LCN (IDs: Zs022_E8-1) with distant terminal branching areas. The whole axon is considered unmyelinated. **B**: AP propagation time maps of the same neuron replotted assuming that axon pieces with a diameter above 0.35 µm are myelinated. The maximum propagation time value in the map is indicated by red, whereas 0 ms is blue on the scale bar next to the particular neuron. Arrows point to regions where the propagation time map shows visible differences. **C**: Propagation time histogram of the axon varicosities of Zs022_E8-1. Bins = 1 ms. Shaded bars, total axon unmyelinated; open bars, axon pieces with a diameter above 0.35 µm are myelinated. *Author's contribution: acquisition of data, 30% contribution.*

Propriospinal connections in the lateral part of the lumbar spinal cord

During the experiments to investigate propriospinal connections, 86 cells were recorded in whole cell mode in the lateral aspect of the spinal dorsal horn and in the LSN. Although post-hoc visualization of biocytin in the recorded neuron was attempted in all cases, successful recovery, that allowed confirmation of the location and classification of the axon and somatodendritic domain, has only been achieved in 32 cases (recovery rate: 37%; *Table 1.*).

Electrophysiological properties and synaptic connectivity

Recorded cells had a mean resting membrane potential of -58.6 ± 1.6 mV (n=84), while the mean input resistance and the membrane time constant were 435 ± 45 MΩ (n=84) and 75.2 ± 10.4 ms (n=56), respectively.

For 54 whole-cell-recorded cells we tested 241 putative presynaptic neurons by cell-attached stimulation (the numbers of trials for a single postsynaptic neuron

cell ID	position	soma / dendrite *(Lima and Coimbra, 1986)*	axon			3-D
			midline crossing	ascending	ipsilateral collaterals	
1	L-I	flattened	AC	c-ALT	DCT	
2	L-I	fusiform	AC	c-ALT	MCT	
3	L-I	flattened	AC	c-ALT	-	
4	L-I	flattened	AC	c-ALT	LCT	
5	L-I	Flattened	-	-	LCN	
6	OUT	NA	AC	c-ALT	-	
7	OUT	pyramidal	AC	c-ALT	MCT	
8	OUT	NA	PC-AC	i-ALT	L-III/IV, L-X	+
9	OUT	NA	PC	c-ALT	L-IV	+
10	OUT	multipolar	-	-	LCN	+
11	OUT	NA	AC	c-ALT	MCT	
12	OUT	NA	AC	c-ALT	DCT	
13	OUT	NA	AC	c-ALT	-	
14	OUT	flattened	AC	c-ALT	LCT	
15	OUT	NA	PC	c-ALT	-	
16	OUT	NA	AC	c-ALT, i-DLF	DLF-caudal, L-I, L-III/IV	+
17	OUT	NA	AC	c-ALT, i-DLF	Lissauer-tract	+
18	OUT	NA	-	-	LCN	
19	OUT	NA	PC-AC	i-ALT	L-III/IV	+
20	OUT	NA	PC-AC	i-ALT	L-III/IV, L-X, L-VII	+
21	OUT	NA	PC	c-ALT	L-I/II	+
22	OUT	NA	PC	c-ALT	L-III/IV*, L-X*	+
23	OUT	NA	AC	c-ALT	MCT	
24	LSN	NA	PC	c-ALT	DLF, L-X	+
25	LSN	NA	AC	c-ALT, i-DF	DLF-caudal	+
26	LSN	NA	AC	c-ALT, i-DF	DLF-caudal	+
27	LSN	NA	PC-AC	i-ALT	-	+
28	LSN	NA	PC	c-ALT	L-VII	+
29	LSN	NA	-	-	LCN	
30	LSN	NA	PC	c-ALT	L-V/VI, L-X	+
31	LSN	NA	AC	c-ALT	MCT	
32	LSN	NA	PC-AC	i-ALT	L-V/VI	+

Table 1. *Position, somatodendritic type and axon trajectory of the recovered neurons*

L-I, lamina I; OUT, between the lateral edge of the dorsal grey and the LSN; LSN, lateral spinal nucleus; NA, not applicable; AC, anterior commissure; PC, posterior commissure; c-ALT, contralateral anterolateral tract; i-ALT, ipsilateral anterolateral tract; DLF, dorsolateral funniculus; DF, dorsal funniculus; L-I-X, lamina I-X; 3-D, neuron reconstructed in three-dimensions with Neurolucida; DCT, dorsal collateral type projection neuron (see *Szücs et al., 2010*); MCT, mixed collateral type projection neuron (see *Szücs et al., 2010*); LCT, lateral collateral type projection neuron *(see Szücs et al., 2010);* blue, neurons with a projection axon crossing in the posterior commissure and ascending in the c-ALT; red, double crossing, i-ALT ascending neurons; green, neurons with bilateral (ipsi and contra) ascending axon

ranged from 1 to 18). Most presynaptic cells tested were selected in the three neighbouring segments caudal to the location of the postsynaptic neuron. *(Figure 8. B-C)*. In 224 cases, stimulation of the presumably presynaptic cell did not evoke response in the postsynaptic neuron. These cells were evaluated as not connected *(Fig 8. C-F)*. The lack of possible mono- or polysynaptic connection was also apparent from the unchanged frequency of excitatory postsynaptic currents (EPSCs) in the 200-ms-long periods before and after the 1ms-long presynaptic stimulation *(Figure 8. D-F)*.

In 12 cases, stimulation of the presynaptic neuron resulted in a reliably evoked EPSC *(Figure 8. D)* with a mean latency of 5.7 ± 1.5 ms (n=12, range of the means: 1.7 – 19.8 ms). The mean amplitude of the monosynaptic EPSCs was 30.7 ± 5.2 pA (n=12, range of the means: 6.6 – 63.4 pA). The stable response caused marked increase in the frequency of EPSCs within the first 50-ms-period after the stimulation *(Figure 8. E-F)*. The occurrence of monosynaptic connections was highest when looking for presynaptic neurons in the first visual field caudal to the postsynaptic recording site and decreased gradually when searching for presynaptic neurons more caudally. The most distant monosynaptically connected neuron was found 4 visual fields (720 μm) away, from the postsynaptic neuron (*Figure 8. C*). This distance is comparable with the length of shorter lumbar segments in the juvenile rat spinal cord.

In case of 5 paired recordings stimulation of the presynaptic neuron initiated a huge increase of the basal EPSC frequency. Interestingly, this was sustained in the postsynaptic neuron for hundreds of milliseconds without further stimulation of the presynaptic cell, possibly due to activation of polysynaptic excitatory pathways *(Figure 8. D)*. For this reason we called this type of connection polysynaptic. A well-defined monosynaptic component in these connections could not be identified due to the complex kinetics of the summed EPSCs *(Figure 8. D)*. When normalized to the EPSC frequency of the 200 ms-long prestimulus period the EPSC increment was highest in the first 50 ms-long bin and showed a gradual decrease unlike the abrupt difference after the first 50 ms period of the monosynaptic connections *(Figure 8. F)*.

Efficacy of the polysynaptic input, electrophysiological properties and synaptic connectivity

We also wanted to see how effective the long-lasting EPSC frequency increase was in evoking action potentials in the 5 neurons receiving polysynaptic input. Thus, we repeated the same protocol (200 ms pre-stimulus and 200 ms post-stimulus periods) in current-clamp mode. The consecutive excitatory postsynaptic potentials (EPSPs) were capable of depolarizing the neurons above the firing threshold even from membrane potentials as low as -90 mV *(Figure 9. A)*. Stimulation of the presynaptic neuron resulted in sustained tonic action potential discharge in the postsynaptic cell held at around -80 mV *(Figure 9. B)*. The frequency of the discharge evoked by this synaptic input stimulation was visibly lower than that evoked by a somatically injected current pulse causing depolarization of similar amplitude, about 10-15 mV *(Figure 9. C)*.

When normalized to the pre-stimulus period, the mean number of action potentials (for all the neurons with polysynaptic input, n=5) showed a 5-fold increase in the poststimulus epoch *(Figure 9. D)*.

From the 5 neurons with polysynaptic input, one (shown in *Figure 9.*) was an LCN in the most lateral part of lamina I with its dendrites protruding mostly into DLF and to a negligible extent into the dorsal horn. Two other cells were outside lamina I but not within the region of the LSN, while the remaining 2 cells were not filled sufficiently for morphological identification.

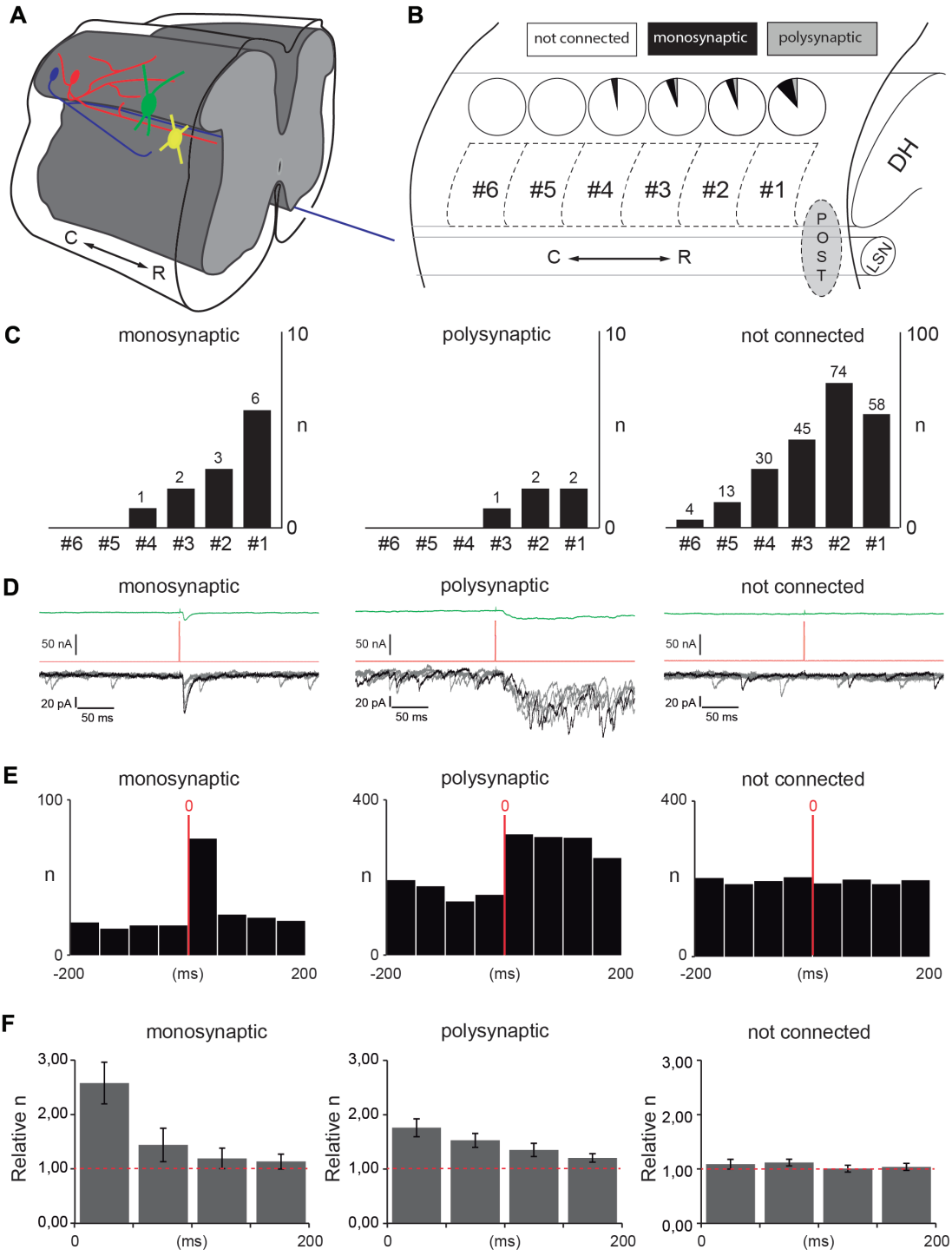

Figure 8. *Short mono- and polysynaptic propriospinal connections of lateral lamina I and LSN neurons*

A: Hypothetic wiring of short propriospinal connections via unmyelinated axons. Lateral axon collaterals of projection neurons (PNs; blue cell) and rostrocaudal axons of local-circuit neurons (LCNs; red neuron) may contact lateral lamina I neuron (green cell) dendrites and LSN neurons (yellow cell) in the dorsolateral funiculus (DLF). **B:** Schematic illustration of the recording regions on the preparation. The grey ellipse represents the region where the postsynaptic neuron was located. Squares shown by dashed lines indicate the different view-

fields. The incrementing numbers refer to the distance from the postsynaptic region. Pie chart above each view-field shows the percentage of neurons with monosynaptic (black) and polysynaptic connection with the postsynaptic neurons. (DH, dorsal horn; LSN, lateral spinal nucleus; POST, postsynaptic neuron; C, caudal; R, rostral). **c)** Number of neurons per view-field that had monosynaptic (left), polysynaptic (middle) or no connection (right) onto the postsynaptic neurons. **D:** Representative voltage-clamp traces of a monosynaptic connection (left), a polysynaptic connection (middle) and a case where the stimulated neuron was not connected to the recorded one (right). In each panel the green trace on the top shows the averaged postsynaptic current, the red trace below shows the cell attached stimulation protocol of the presynaptic neuron (200 ms long recordings before and after the 1-ms current step injection into the presynaptic neuron). Bottom traces show 5 non-consecutive individual voltage traces recorded in the postsynaptic neuron (for clarity one is highlighted in black). **E:** Cumulative number of excitatory postsynaptic currents (EPSCs) from 90 consecutive traces in 50-ms-bins before and after the transient stimulation of the presynaptic neuron in case of a monosynaptic pair (left), a polysynaptic connection (middle) and in a case where the stimulated neuron did not evoke a response in the postsynaptic one (right). Red vertical lines indicate the time point (0 ms), when the presynaptic neuron was stimulated. Note the differences on the Y axis. **F:** Normalized cumulative EPSC numbers from 90 consecutive trials in 50 ms-bins following stimulation in monosynaptic pairs (left, n=8), polysynaptic connections (middle, n=5) and cases where the neurons were not connected (right, n=5). The red dashed line indicates the average number of EPSCs recorded during the 200 ms period preceding stimulation.

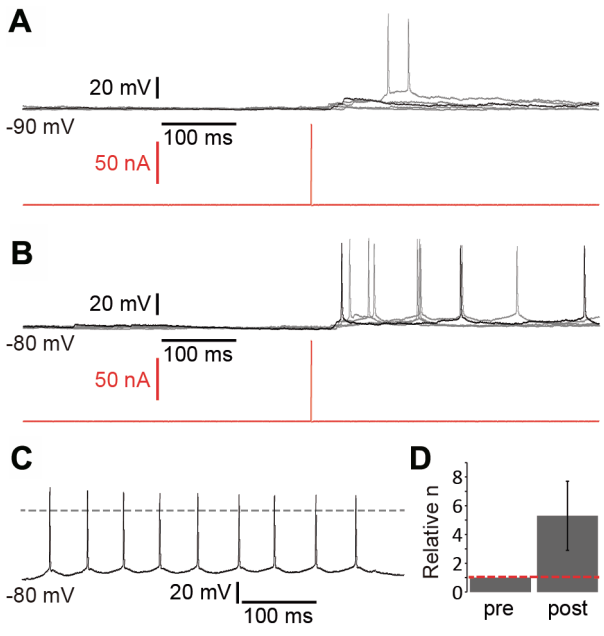

Figure 9. *Functional efficacy of polysynaptic connections*

A: Voltage responses (top; one highlighted trace in black and 4 consecutive traces in grey) of a lateral lamina I local-circuit neuron kept around -90 mV with injected hyperpolarizing current in response to transient suprathreshold stimulation of the presynaptic neuron (bottom; in red). **B:** The same neuron on a more depolarized membrane potential (around -80 mV) showed increased spike discharge in the post-stimulus period. **C:** Spike discharge pattern of the same neuron upon 40 pA depolarizing current injection. Dashed line indicates the 0 mV level. **D:** Normalized pre- and poststimulus spike numbers for all 5 neurons showing polysynaptic response to single presynaptic neuron stimulation.

Morphology of neurons in the LSN and in the lateralmost aspect of lamina I

General somatodendritic features of neurons outside the dorsal grey matter

From the 32 neurons, in which biocytin was successfully recovered, only 5 cells were located within the boundaries of lamina I *(Table 1.)*. The rest of the cells were next to the lateral edge of lamina I, among the superficial fibres of the DLF (n=18) or within the LSN (n=9). While neurons within lamina I could be classified according to the system introduced by *Lima and Coimbra (1986)*, neurons located more laterally, outside the dorsal grey matter and in the LSN, with the exception of three cells *(Table 1.)* presented very different somatodendritic features.

We compared basic morphometric parameters of these neurons with a pooled sample of 3-D reconstructed projection neurons (PNs) from the work of Luz and colleagues *(Luz et al., 2010)* and LCNs from our earlier study (see chapter on "*Morphology of local circuit neurons in lamina I" and corresponding publication*; n=4 for each). Neurons lateral to lamina I and in the LSN had more stem dendrites *(Figure 10. D)* and significantly longer total dendritic length (summed dendritic segment length; *Figure 10. E; $p<0.05$, Student´s t-test*). This difference was apparent in the generally more "bushy" appearance of neurons outside lamina I *(Figure 10. A-B)*. Another striking feature of the neurons lateral to lamina I was the presence of numerous short spines along the dendritic surface *(Figure 10. B-C)*. In some cases spines appeared to be present even on the neuronal soma itself *(Figure 10. B)*. Indeed, the total number of spines and spine density both proved to be significantly higher in neurons outside lamina I (OUT/LSN, *Figure 10. F-G; $p<0.01$ and $p<0.05$ respectively, Student´s t-test*).

Distinct axon trajectories of neurons outside lamina I and in the LSN

Regardless of the location of their somata, the recovered neurons could be grouped into distinct categories on the basis of the type and course of their axons *(Table 1.)*. 16 out of 32 successfully recovered neurons (cells 1-7, 10-14, 18, 23, 29 and 31) could be classified according to earlier published criteria for projection- and local-circuit neurons *(Szücs et al., 2010)*. Regular projection neurons gave rise to a single projection axon that originated from the cell body or one of the primary dendrites, crossed the midline in the anterior commissure and ascended in the contralateral anterolateral column (c-ALT). Some of these neurons had collaterals

that fell into groups that were previously described in lamina I *(Szücs et al., 2010)*.

In 7 cases (cells 9, 15, 21-22, 24, 28 and 30; blue cells in *Table 1.*) the main axon crossed the midline in the posterior commissure and shortly after entered the medial side of the contralateral anterior column where it started to ascend.

Another set of neurons (cells 8, 19-20, 27 and 32; n=5, red cells in *Table 1.*) had axons with a similar initial course, but instead of ascending on the contralateral side these axons returned to the ipsilateral side by re-crossing in the anterior commissure and exited into the medial part of the ipsilateral anterior funiculus.

Finally, the main axon of the remaining 4 cells (cells 16-17 and 25-26; green in *Table 1.*), before crossing the midline in the anterior commissure and ascending in the c-ALT, gave rise to two long axon branches one of which ascended in either the ipsilateral DLF (i-DLF) or the ipsilateral dorsal funiculus (i-DF), while the other, showing characteristic features of unmyelinated collaterals, descended in the i-DLF. Although the major grouping criterion was the axon trajectory, neurons divided on this basis also showed other common characteristics described below.

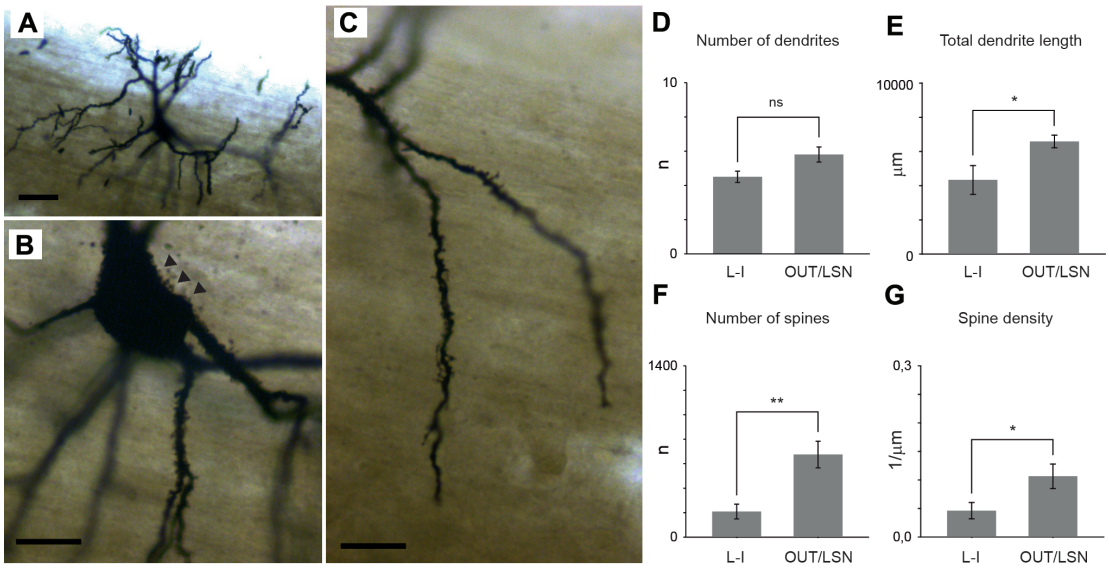

Figure 10. *Somatodendritic characteristics of neurons outside lamina I and in the LSN*
A: Low magnification photograph of a neuron (cell 24 in Table 1) in the LSN, giving rise to numerous not too long, frequently branching dendrites organized in a multipolar fashion. **B-C:** Dendrites were densely covered with short spines, and spine-like protrusions which were also encountered on certain parts of the soma contour (arrowheads). Scale bars: a, 50 µm; b-c, 20 µm. **D:** Mean number of dendrites in an earlier lamina I sample of projection and local-circuit neurons (L-I; n=8; Luz et al., 2010; Szücs et al., 2013) and cells lateral to the border of the grey matter and in the LSN (OUT/LSN, n=15). **E:** Mean total dendrite (reconstructed dendritic segment) length in the same groups of neurons. **F:** Mean total number of spines encountered on the dendrites of neurons in the two groups. **G:** Mean spine density (total number of spines / total dendrite length) in the two neuron groups. *, $p<0.05$; Student´s t-test; **, $p<0.01$, Student´s t-test

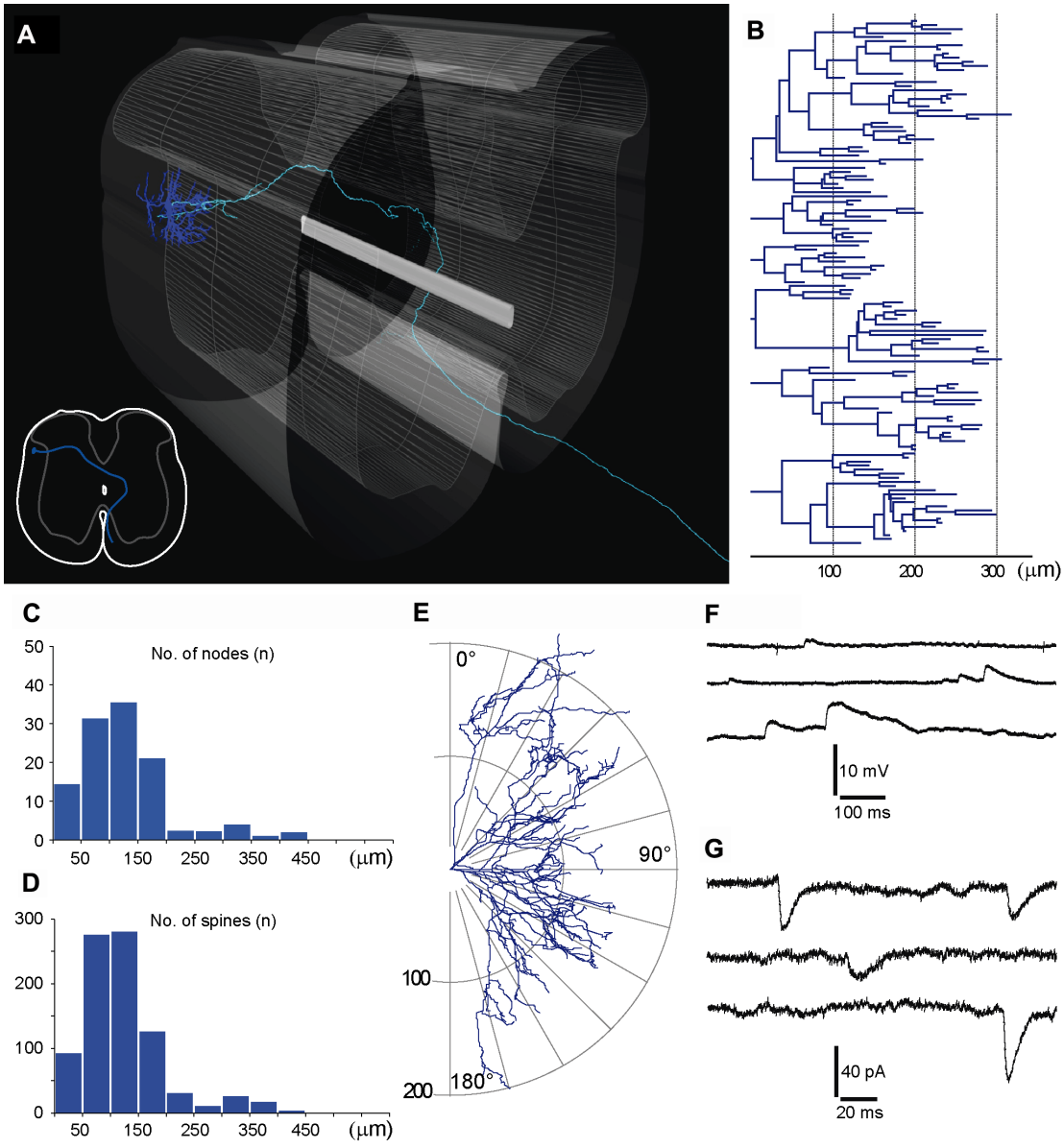

Figure 11. *Morphological description of neurons with their projection axon crossing in the posterior commissure*

A: Three dimensional reconstruction of the neuron (cell 24 in *Table 1*. also shown on the photographs in *Figure 10.*) positioned in a schematic spinal cord block. Inset shows trajectory of the axon in the transverse plane, crossing the midline in the posterior commissure and exiting into the white matter on the medial side of the anterior column. **B:** Dendrogram of the same neuron showing a compact dendritic tree with dense branching in the vicinity of the soma. **C-D:** Sholl analysis of the distribution of nodes (branchpoints) and spines of the neuron shown in panel A. **E:** Fan-in diagram of the same neuron. Dendritic processes cover the whole angle-range, showing no preferred orientation. **F:** Spontaneous EPSPs recorded at zero injected current in current-clamp mode from three different neurons within this group. **G:** Voltage-clamp recordings from the same neurons. The blue color used in the figure refers to the color-code of this cell-group in *Table 1.*

Posterior commissural contralaterally projecting neurons

Neurons belonging to this group showed a spherical organization of their dendrites with the cell body located on the most superficial part rather than the center of this spherical structure. Dendrites protruded out from the soma in a multipolar fashion and occupied a large part of the DLF *(Figure 11. A)*. Dendrites branched frequently even in the vicinity of the soma, thus dendritic segment were generally short *(Figure 11. B-C)*.

This type of neuron possessed a high number of short spines *(Figure 11. D)*. Fan-in projection revealed that dendrites showed no preferred orientation filling the space around the soma equally *(Figure 11. E)*.

The axon of these neurons started off medially from the soma or proximal dendrites, entered the grey matter and aimed medially towards the central canal. The main axon gave collaterals on the ipsilateral side to various laminae, including lamina X around the central canal *(Table 1.)*, and crossed the midline in the posterior commissure. The axon on the contralateral side took a short path ventrally before it exited into the medial side of the anterior column white matter *(Figure 11. A)*.

Examination of the spontaneous synaptic input to these neurons revealed occasional, long-lasting and large amplitude EPSPs *(Figure 11. F)* and EPSCs *(Figure 11. G)*. Summation of these spontaneous events showing generally slow kinetics was not observed.

Double crossing ipsilaterally projecting neurons

In the sample of neurons with unique axon trajectories 5 neurons possessed a main axon that crossed the midline twice *(Figure 12. A)*.

Dendritic arborisation of these cells were also dense with numerous branch points close to the soma *(Figure 12. B-C)* and they also presented a high number of spines *(Figure 12. D)*, although less, than neurons crossing in the posterior commissure. However, the orientation of the dendrites was more restricted: they were either going dorsally and followed the curvature of the dorsal grey matter, occupying mostly lamina I-II, or turned ventrally and branched in the DLF. For this reason Fan-in projection showed marked accumulation around 90 degrees *(Figure 12. E)*.

The axon started off in the medial direction and aimed towards the posterior commissure giving ipsilateral collaterals in laminae of the deep dorsal horn, intermediate grey matter and around the central canal (lamina X). Interestingly none

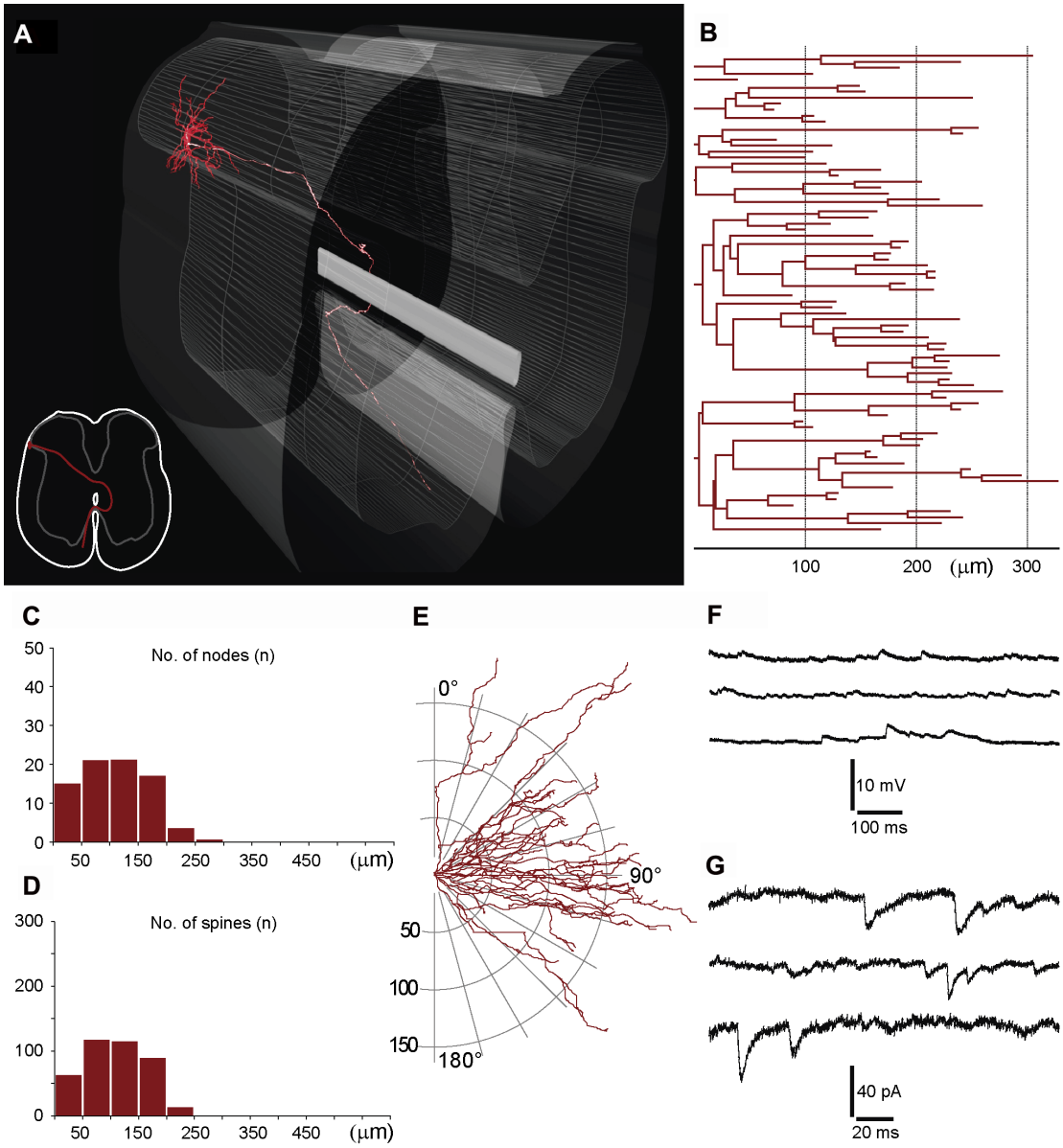

Figure 12. *Morphological features of neurons with double midline crossing ipsilateral projection axon*

A: Three dimensional reconstruction of a neuron (cell 27 in *Table 1.*) just outside lamina I, at the lateral edge of the dorsal grey matter. Inset shows trajectory of the axon in the transverse plane. The single projection axon of the cell crosses the midline first in the posterior commissure and re-crosses again in the anterior commissure. The axon then enters the white matter in the medial aspect of the anterior column. **B:** Dendrogram of the same neuron showing a relatively compact dendritic tree with less branching than in case of neurons in *Figure 11.* **C-D:** Sholl analysis of the distribution of nodes (branchpoints) and spines of the same neuron. **E:** Fan-in diagram of the same neuron. Dendritic processes show some preference for the vertical (dorso-ventral) direction, which is apparent from the slight accumulation of processes around 90 degree. **F:** Spontaneous EPSPs recorded at zero injected current in current-clamp mode from three different neurons within this group. **G:** Voltage-clamp recordings from the same neurons. The red color used in the figure refers to the color code of this cell-group in *Table 1.*

of the 5 neurons gave collaterals to the superficial dorsal horn. The main axon then crossed the midline in the posterior commissure, took a short loop on the contralateral side and re-crossed in the ventral commissure to enter the medial aspect of the white matter in the ipsilateral anterior column *(Figure 12. A)*.

Spontaneous synaptic input was more frequent than in the posterior commissure crossing cell group; both EPSPs and EPSCs were showing faster kinetics and occasional summation *(Figure 12. F-G)*.

Bilaterally projecting neurons

Finally, 4 neurons, two in the LSN and two between the LSN and the edge of the dorsal grey, presented a main axon, that before crossing the line in the anterior commissure, gave rise to an equally strong myelinated-appearing (for criteria see *Figure 6.*) axon branch that entered and ascended in the i-DF or i-DLF. Another characteristic morphological feature was the presence of single thin ipsilateral axon collaterals that had numerous varicosities and descended in the DLF or Lissauer´s tract *(Table 1.)*. A typical neuron of this type is shown in *Figure 13. A*.

The dendritic tree is quite asymmetric, having most branches filling a conical space in the DLF and having a single branch that spreads medially *(Figure 13. A)*. Dendrites were more extensive and branched less frequently than in case of the previous two groups, resulting in longer and less dendritic segments *(Figure 13. B-C)*. Spines were less numerous, not exceeding the values observed earlier in case of neurons in lamina I *(L-I, Figure 10.)*. Fan-in projection confirmed the conic arrangement of dendrites in DLF, showing a prominent accumulation of dendrites at 90 degrees *(Figure 13. E)*.

Interestingly, despite the fact that these cells had few spines, the frequency of spontaneous excitatory activity was high and all cells in this group showed large number of various amplitude EPSPs and EPSCs that were often superimposed *(Figure 13. F-G)*.

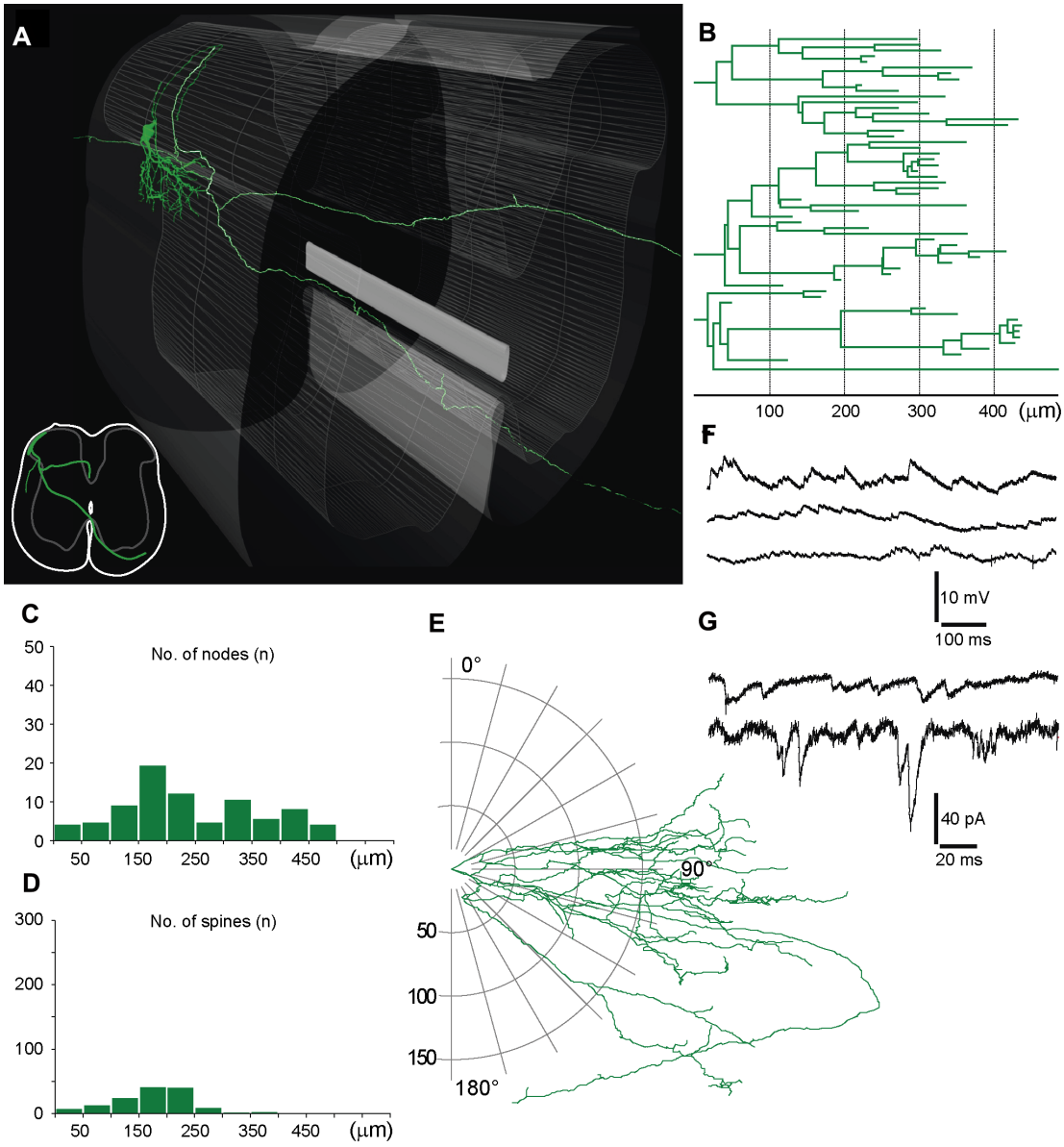

Figure 13. *Morphological description of neurons with bilateral projection axon*
A: Three dimensional reconstruction of a typical, very asymmetric neuron (cell 26 in *Table 1*) in this group. Inset shows trajectory of the axon that, in this case, originates from the single long dendrite that follows the curvature of the dorsal horn. The main axon then splits into two and enters the ipsilateral DF and contralateral anterior column. **B:** Dendrogram of the same neuron showing long, slender sparsely branching dendrites. **C:** Sholl analysis of the distribution of nodes (branchpoints) and spines **(D)** of the neuron shown in panel a. **E:** Fan-in diagram shows a major preference of dendrites to the vertical direction, with most dendrites reaching ventrally into the DLF. **F:** Numerous fast spontaneous EPSPs recorded at zero injected current in current-clamp mode from three different neurons within this group. **G:** Voltage-clamp recordings from the same neurons. The green color used in the figure corresponds to the color code of this cell-group in *Table 1*.

Differences in spontaneous EPSC and EPSP frequency and kinetics of distinct morphological neuron types

In order to quantitatively analyze the differences in the frequency of spontaneous postsynaptic events (sEPSCs and sEPSPs) we selected, from each neuron 10 traces (length: 200-800 ms) where the presynaptic neuron was not stimulated, calculated the sEPSC frequency for each trace and presented pooled data for the corresponding groups in *Figure 14* (n=70, blue; n=40, green; n=40, red). Statistical analysis proved that bilaterally projecting neurons presented a significantly higher (p<0.05, Kruskal-Wallis One Way Analysis of Variance on Ranks followed by Dunn´s Pairwise Multiple Comparison) mean frequency (23.4 ± 2.1 Hz) of spontaneous events than neurons with the other two types of axonal trajectories (6.6 ± 1.1 Hz, blue; 6.4 ± 1.3 Hz, red; *Figure 14. A*).

For measurements of sEPSP and sEPSC kinetics descriptions we selected 7-30 events of each type for each neuron in a given group (sEPSPs: n=67, blue; n=40, green; n=40, red; sEPSCs: n=163, blue; n=60, green; n=90, red). Spontaneous EPSCs were taken from traces where the presynaptic neuron was not stimulated, while sEPSPs were analyzed using current-clamp traces of the firing pattern protocol (at 0 current step) acquired for each cell. The mean amplitude of sEPSCs was significantly smaller (p<0.05, Kruskal-Wallis One Way Analysis of Variance on Ranks followed by Dunn´s Pairwise Multiple Comparison) in neurons with double crossing ipsilaterally projecting axon (17.6 ± 0.9 pA, red cells; 30.4 ± 1.7 pA, blue neurons; 32.1 ± 3.5 pA, green cells; *Figure 14. B, F*). The mean sEPSP amplitudes, however, did not show significant differences (1.3 ± 0.1 mV, blue; 1.1 ± 0.1 mV, red; 1.3 ± 0.2 mV, green; *Figure 14. C*). Mean rise time (measured as time-to-peak) was significantly shorter (p<0.05, Kruskal-Wallis One Way Analysis of Variance on Ranks followed by Dunn´s Pairwise Multiple Comparison) in bilaterally projecting neurons for both sEPSCs (2.0 ± 0.1 ms, green; 3.1 ± 0.1 ms, blue; 3.3 ± 0.1 ms, red; *Figure 14. D*) and sEPSPs (4.1 ± 0.4 ms, green; 8.8 ± 0.4 ms, blue; 7.1 ± 0.4 ms, red; *Figure 14. E*). The obvious difference in the sEPSC kinetics of averaged traces *(Figure 14. F)* could be best demonstrated after scaling to the same amplitude *(Figure 14. G)*.

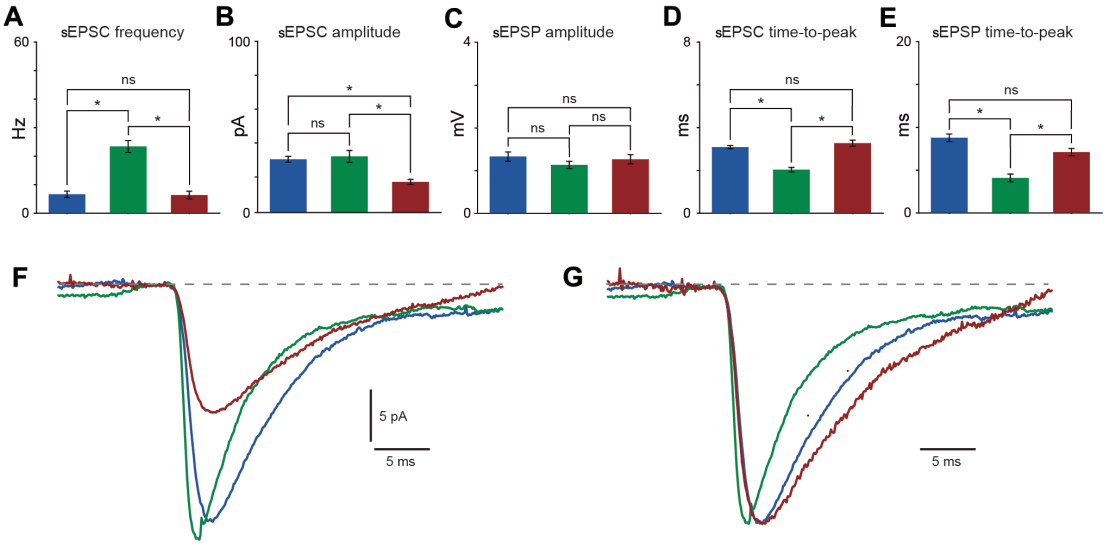

Figure 14. *Comparison of spontaneous EPSCs and spontaneous EPSPs in the three axon trajectory groups*

Colors of the traces and bars used in the graphs correspond to the color codes of the cell-groups in Table 1. **A:** Mean sEPSC frequency was significantly higher in neurons with bilateral axon (green). **B:** Neurons with double midline crossing ipsilateral projecting axons showed sEPSCs with significantly lower mean amplitude (see also **F**). **C:** There was no difference in the mean amplitude of sEPSPs between neurons in the three groups. **D-E:** Mean rise time (measured as time-to-peak) of sEPSCs and sEPSPs was significantly shorter in neurons with bilateral axon (green). **F:** The difference in EPSC kinetics is shown on averaged baseline-adjusted and aligned traces **G:** and became more obvious when averaged traces of the three groups were scaled to the same amplitude. Colors of the traces and bars used in the graphs correspond to the color codes of the cell-groups in Table 1. *, $p<0.05$; Kruskal-Wallis One Way Analysis of Variance on Ranks with Dunn´s Pairwise Multiple Comparison.

DISCUSSION

The experimental results described in the publications presented in this thesis have shown that LCNs frequently possess a number of short and putative long propriospinal branches, and this feature provides morphological basis for their possible involvment in segmental interlaminar and propriospinal sensory information processing. We have also tested the hypothesis that rostrally oriented axons in the DLF, comprising, in part, the collaterals of PNs as well as local axon of LCNs, are providing synaptic input to dendrites of lateral lamina I neurons and to neurons located in the LSN. We proved that stimulation of superficial cells in the lateral aspect of lamina I could indeed evoke mono- and polysynaptic excitation of LSN and lateral lamina I neurons, although these connections were rare. On the other hand, by careful 3-D reconstruction of the neurons, we discovered, and described for the first time, previously undescribed axon trajectories of putative projection or propriospinal neurons in the lateral dorsal spinal cord.

Technical considerations

Regarding our morphological results, it has to be noted that our sample is biased in some respects. First we used young animals, because the viability of the in vitro intact spinal cord preparation in our experiments proved to be best at the age of P14–P24. For this reason, one cannot exclude the possibility that axons of more mature dorsal horn neurons may be different. This, however, seems unlikely, as lamina I neurons with very similar local axon branching pattern have been described for adult rats *(Li et al., 2000)*. Second, because of the decreased visibility through regions rich in myelinated fibers, the medial part of the dorsal horn surface (dorsal root entry zone) was excluded from the search for neurons. Thus, conclusions of this study are based on neurons from the lateral two-thirds of lamina I in case of LCNs and the lateral edge of lamina I as well as superficial neurons scattered among the fibers of the DLF. Third, when we visualized the surface of the dorsal horn in our intact spinal cord preparation, detection of the laminar border between lamina I and substantia gelatinosa relied solely on the appearance of the uniform, densely packed layer of small lamina II neurons. For this reason, to ensure that recorded neurons were in lamina I, we selected larger neurons in the most superficial (first to appear)

cell layer of the dorsal horn. In this way we unavoidably excluded small lamina I neurons. Finally, full analysis of all investigated parameters was possible only in 3-D reconstructed neurons. However, the number of such reconstructions is relatively small compared with the total number of neurons in our sample in case of LCN neurons, resulting in an additional source of potential variance. At the same time the sample of 3-D reconstructed neurons from both studies have substantially increased the number of spinal cord neurons in a widely used and well-established neuronal morphology database (Neuromorpho.Org) after receiving a request to donate them to the database. This way neurons from these studies will be useful tools for future theoretical and computational studies. Our submitted neurons are presently being processed for publication by the database technicians.

The morphological recovery rate in case of neurons in the lateral aspect of the spinal dorsal horn and in the LSN was somewhat lower (37%) than in case of LCNs in the lateral two-thirds of lamina I. This might be due to the increased difficulty of maintaining proper seal conditions among the fibres of the DLF. Nevertheless, this is still higher than the success rate of recovering biocytin filled cells in the LSN (30%), reported by Pinto and colleagues *(Pinto et al., 2010)*. Probably due to the same reason, we could not achieve presynaptic labelling to an extent that would have allowed identification of synaptic connections in the initial trials, thus, later we excluded biocytin from the cell-attached pipette to reduce contamination of the preparation that would have made it difficult to trace the axon trajectories.

Unlike most paired recordings from visually identified neurons where the connected neurons are usually located in the same visual field, we aimed to investigate monosynaptic connections between cells that were remotely located. Even though we used cell-attached stimulation of putative presynaptic neurons, advancing the visual field while keeping the selected postsynaptic neuron in proper whole-cell configuration was very challenging. We continuously monitored the condition of the postsynaptic neuron, but one cannot exclude the possibility that some connections may have been overlooked when evoked event amplitudes fell below detection level due to the progressive deterioration of the seal. Thus, ratios reported here for mono- and polysynaptic propriospinal connections may be underestimations.

The technically challenging recording configuration also required experimentation with young adult animals that are regularly used in electrophysiological studies in vitro. While the possibility that short propriospinal

connectivity rate may be different in older animals cannot be excluded, it is unlikely that anatomical features such as collaterals embedded in the dense fibre bundles of the DLF would change significantly. Midline crossing of the main axon that is only limited to a short time window during development is even less likely to be altered during further maturation of the animal.

Possible roles of LCNs in local neuronal networks of the dorsal horn

The extensive branching of LCN axons suggest that, besides the anatomical divergence of primary afferent fibers, LCNs may provide further divergence of processed primary afferent information after integrating it with other sources of input. Furthermore, LCN axons occupy most dorsal laminae (I–II and occasionally III–IV), and this feature, theoretically, allows relaying of C-fiber information to deeper laminae. Indeed, Braz and Basbaum *(Braz and Basbaum, 2009)* reported neurons in deep laminae (III–V) receiving polysynaptic input from unmyelinated primary afferents. Lamina I LCNs may be direct sources of such polysynaptic input or provide it through contacting lamina II islet and stalked neurons that were shown to project to deeper laminae *(Eckert et al., 2003).* At the same time, multipolar LCNs may be monosynaptically activated by primary afferents that terminate in deeper laminae. Consequently, neurons in laminae III–V may integrate direct primary afferent information with indirect processed form of the same information through lamina I LCNs.

Because of their extensive local axon, we can also presume, that relatively few LCNs could influence the superficial dorsal horn along several segments, in a sustained tonic manner based on their firing pattern and the frequent occurrence of rhythmic intrinsic firing. The large number of varicosities and the highly branched, extensive axon of LCNs also imply that these neurons may be involved in volume transmission.

Possible roles of LCNs in short and long propriospinal neuronal networks

A large percentage of LCNs (86% of flattened and 69% of multipolar neurons) had long, solitary axon branches, often with a myelinated appearance, in the DF, DLF and Lissauer's tract. These branches often ran for two to three segments in the rostrocaudal direction without any preferential direction, and then they faded

below visibility. Similar axon branches originating from lamina II-III neurons have already been described in the dorsolateral white matter by earlier anatomical studies *(Lenhossék, 1895; Cajal, 1909; Szentágothai, 1964),* and intersegmental integration was also proposed recently for dorsal horn cholinergic neurons, with similar rostrocaudal axonal organization *(Mesnage et al., 2011)*. However, morphological features of LCNs in our sample imply, that they can also act as short and in some cases as long propriospinal neurons.

The presence of such collaterals is also in line with electrophysiological observations. About one-third of nociceptor-driven lamina I neurons could be antidromically activated by stimulation of Lissauer's or deeper tracts from up to three segments rostral to their origin *(Cervero et al., 1979)*. The conduction velocity of the axons of these neurons suggested that they are small and myelinated *(Cervero et al., 1979).*

It also has to be noted, that while in the superficial dorsal horn all LCNs had collaterals (reaching I-II, occasionally entering lamina III and IV), and only around one third of ALT-PNs *(Szücs et al., 2010),* at the same time, the contribution to rostrocaudallly oriented varicose axon collaterals from the two groups is more balanced in the DLF: 39% of LCNs and 40% of ALT-PNs (lateral and mixed collateral types) have collaterals in this region. Therefore, we can assume that besides the previously described lamina II and III neurons, both LCNs and ALT-PNs of lamina I may contribute to relaying local segmental information to neighboring segments and to neurons of the LSN.

Functional consequences of the organization of LCN axons: branching, varicosity distribution and spike propagation

Temporal dispersion of synaptic input is of crucial functional importance in case of complex axon arbors bearing thousands of varicosities, forming networks in the highly somatotopic spinal dorsal horn. The propagation time of an AP, initiated in the axon initial segment, is determined mostly by path length, axon diameter, myelination, and branching *(Debanne et al., 2011)*.

Path distance to a particular point of the axon is strongly dependent on branching. The alternating branching of primary collaterals from the main axon into the rostral and caudal directions, frequently observed in this study, seems to be an

efficient solution for maximally filling the target space (laminae I–III) and, at the same time, equalizing path distance for the rostral and caudal portions of the axon tree. This setup, however, in a system with strong spatial boundaries, such as the spinal dorsal horn, results in an overlap between major branches. Target regions supplied by multiple overlapping branches may be activated repeatedly.

Short intersegmental connections of lamina I and the LSN are rare but some may be very potent

As a result of our electrophysiological experiments we have demonstrated that neurons outside the dorsal grey matter and in the LSN receive monosynaptic connections from lateral lamina I neurons. Connected neurons were rare and could not be detected at distances above 720 micrometres in the caudal direction. Such connections may be considered as intersegmental, since upper lumbar segments in animals of the experimental age we used have similar lengths.

In terms of functionality, these ultra-short propriospinal connections are of questionable importance, but may increase the complexity of intraspinal divergence and convergence *(Pinto et al., 2010)* of primary afferent inputs. Synaptic delay in the recorded monosynaptic connections showed a large variation, but even the longest observed latencies would be compatible with putative long axodendritic pathways and recording conditions at room temperature *(Luz et al., 2010)*.

At the same time, a striking observation in this study was the presence of powerful polysynaptic excitation of some neurons in the DLF region. The stimulation of a single presynaptic lamina I neuron evoked long-lasting and suprathreshold excitation of postsynaptic cells. A putative circuitry behind such phenomenon would include a set of excitatory interneurons that spread and amplify the activity of a single "initiator" neuron via feedforward excitation. The sustained EPSC frequency increase may also be explained by a powerful inhibition of inhibitory interneurons, thus, via disinhibition, the normally silent but now liberated excitatory neurons could be responsible for the frequency increase of EPSCs in target neurons. This mechanism would require a long-lasting inhibition upon a single transient - although suprathreshold - stimulation of the presynaptic "initiator" neuron. These "initiator" neurons may also be involved in pathological amplification of incoming signals during certain chronic pain conditions, thus identification of them would be crucial.

A good candidate for the "conductor" neuron would be those excitatory and inhibitory LCNs in lamina I that have extensive axons that bridge several segments rostrocaudally and have thousands of varicosities, making them capable of providing high excitatory or inhibitory transmitter levels in a large volume of the spinal dorsal horn. Unfortunately, in this study, the insufficient quality of labelling in pre-synaptic neurons prevented us to elucidate this question.

Neurons in the lateral aspect of the dorsal horn show morphological evidence for integration

With the exception of 5 cells the majority of neurons in the recovered sample fell outside the dorsal grey matter, some clearly within the boundaries of the longitudinal cell column of the LSN, while others between the edge of the dorsal grey and the LSN.

In general organization of the dendrites was very different from PNs and LCNs of lamina I. Neurons close to the dorsal grey were asymmetric having most dendrites protruding into the DLF ventrolaterally, and only a few aimed to the medial direction, running close to the surface within lamina I (see neuron in *Figure 13. A*). Earlier morphological studies in the LSN described neurons with dendrite oriented either laterally *(Bresnahan et al., 1984; Rethelyi, 2003)*, medially *(Menetrey et al., 1982; Rethelyi, 2003)* or rostrocaudally *(Rethelyi, 2003)*. LSN neurons in our sample showed a combination of these features and were either spherical (e.g. the neuron in *Figure 11. A*) or had two main groups of dendrites going ventrolaterally and dorsally (e.g. the neuron in *Figure 12. A*), filling the DLF almost completely. This difference may be due to the incomplete or random labelling of neuronal processes with the methods used in the previous studies (e.g. Golgi-Kopsch method).

Above the dense arborization of dendrites in the DLF, these lateral neurons also possessed a high number of dendritic spines, further increasing the putative contact surface. This efficient coverage of the DLF cross section is in line with the suggestion of *Olave and Maxwell (2004)* that the LSN may function as an integrative nucleus, where neurons can receive inputs from primary afferents of visceral origin, interneurons and descending pathways from supraspinal loci.

Axonal architecture of neurons outside the superficial dorsal grey matter

It has long been known that neurons of the LSN can be retrogradely labelled from various supraspinal loci, including the parabrachial nucleus *(Ding et al., 1995; Feil and Herbert, 1995)*, the periaqueductal grey *(Pechura and Liu,1986; Harmann et al., 1988)* the nucleus of the solitary tract *(Menetrey and Basbaum, 1987; Esteves et al., 1993)*, the medullary reticular formation *(Leah et al., 1988; Pechura and Liu, 1986)*, the nucleus accumbens, the septum *(Burstein and Giesler, 1989)* and the amygdala and orbital cortex *(Burstein and Potrebic, 1993)*. LSN neurons project bilaterally to the mediodorsal thalamic nucleus and some authors assume that this LSN-mediodorsal pathway may be involved in the emotional and cognitive aspects of pain *(Gauriau and Bernard, 2004)*.

The above morphological evidence implies that the majority of LSN neurons are projection neurons, and this view is also supported by *Réthelyi (2003)*, who observed that the axons of LSN neurons become myelinated soon after their origin; a common feature of projection axons *(Réthelyi, 2003)*. Besides supraspinal targets, LSN neurons also project to lamina I, II, V and VII of the spinal cord *(Jansen and Loewy, 1997)*.

In good agreement with the above, in this study we found that most neurons outside the dorsal grey matter (24 out of 27) - including LSN neurons - had a myelinated-appearing projection axon and 20 had ipsilateral collaterals within almost all laminae of the spinal grey matter. Despite this fact one cannot rule out the possibility that some of these cells could be propriospinal neurons, since axons running in the anterolateral funiculus were shown to form inter-enlargement pathways between the cervical and lumbar spinal cord *(Reed et al., 2006)*. Furthermore, contralateral lumbosacral lamina I neurons have been retrogradely labelled after tracer injections into the cervical ventral horn and some of them look very similar to bilaterally projecting cells of our study *(Figure 1. I in Dutton et al., 2006)*. Such labelling however could have resulted from uptake of tracer by projection neuron axons of passage, located in the same anterolateral funiculus *(Dutton et al., 2006)*. Thus, further experiments with prior retrograde labelling of projection neurons from supraspinal centres will be needed to clarify the exact function of the neurons described in our study.

Similarly to earlier observations *(Szücs et al., 2010)* dendritic origin of the axon was also frequent among neurons outside lamina I and in the LSN. The most

remote axon initiation (~90 μm) occurred in one of the bilaterally projecting neurons, (shown in *Figure 13. A)* where the axon originated from the single medially oriented loopy dendrite. This observation enforces earlier results of computer simulations *(Lee et al., 2005)* and suggestions *(Szücs et al., 2010)* that both the distal and proximal part of the dendrite giving rise to an axon may have very important roles in the regulation of action potential initiation. Indeed, with the help of modern techniques, in a recent study authors provided functional evidence for the influence of dendritic axon origin on action potential initiation *(Thome et al., 2014).*

Projecting axon of neurons located outside the dorsal grey matter may also cross the midline in the posterior commissure

The mechanisms that govern axon midline crossing during development have been well studied, particularly at the level of the spinal cord *(Escalante et al., 2013).* Attracting and repellent factors such as BMP7, Netrin1 and Sonic-Hedgehog, secreted by the floor-plate and roof-plate were shown to act in a complementary and sequential manner to guide sets of axons within the developing CNS *(Augsburger et al., 1999).*

While lamina I projection neurons in earlier works *(e.g. Szücs et al., 2010),* without exception, crossed the midline in the anterior commissure, neurons outside the dorsal grey matter and in the LSN showed other axon trajectories. In 7 cases the main axon crossed the midline in the posterior commissure and continued to ascend in the medial part of the anterior column white matter. These axons may be among those reported by *Petkó and Antal (2000)* crossing the midline in the posterior commissure after BDA injection into the lateral part of lamina III and IV, where the anterograde tracer may have been picked up also by neurons located in the DLF.

Midline crossing in the posterior instead of the anterior commissure may be the result of different responsiveness of the path-finding axon cone or a temporal difference in neuronal development that results in missing the time window for regular crossing in the anterior commissure. Anterograde tracing of posterior commissure crossing axons will be important to define targets and function of these neurons.

Axon trajectory of double crossing ipsilaterally projecting neurons oppose our present knowledge on axon midline guidance

The finding that five neurons in our sample possessed axons that ascended in the ipsilateral white matter is not striking in itself, since lamina I neurons, most of them belonging to the multipolar somatodendritic type, have been reported to be projecting ipsilaterally to the dorsal reticular nucleus *(Lima, 1998)*. On the other hand, the fact that the projection axon in these 5 cases crosses the midline twice is not compatible with our present knowledge on axon midline guidance.

Prior to midline crossing, comissural axons are attracted by floor plate-derived Netrin-1 and Sonic Hedgehog *(Kennedy et al., 1994; Charron et al., 2003).* After crossing, repellents of the Slit and Semaphorin families expel axons from the floor plate and prevent re-crossing *(Zou et al., 2000; Long et al., 2004)*. Slits act through receptors of the Robo receptor family. Robo3, which is expressed exclusively in commissural neurons, produces two splice isoforms with opposite activities *(Sabatier et al., 2004; Chen et al., 2008)*. Robo3.1 is expressed on pre-crossing axons and suppresses premature responsiveness to Slits, thereby allowing midline crossing; Robo 3.2 localizes to post-crossing axons and acts as a classical Slit receptor that contributes to midline repulsion *(Chen et al. 2008)*, thus rendering recrossing impossible.

In this paper, however, we show, for the first time, that there are ipsilaterally projecting neurons that cross the midline twice: first in the posterior commissure and then, after taking a short path in the contralateral grey, for a second time in the anterior commissure. Although the molecular program that determines axonal ipsilaterality in the spinal cord is poorly understood, recently, ipsilateral neurons whose axons grow in close proximity to the midline, such as the ascending dorsospinal tracts and the rostromedial thalamocortical projection, were demonstrated to avoid midline crossing because they transiently activate the transcription factor Zic2. In contrast, uncrossed neurons whose axons never approach the midline control axonal laterality by Zic2-independent mechanisms *(Escalante et al., 2013).* This explanation, however, implies that ipsilateral axons stay on the same side without crossing the midline. Our observation suggests that there are other, yet unresolved molecular mechanisms that govern axon crossing through the midline. Further tracing and lineage analysis studies will be necessary to elucidate the function and origin of these neurons.

Bilaterally projecting axons

Apart from the neurons with posterior commissure crossing and double-crossing projecting axons, 4 cells had bifurcating myelinated-appearing axons. The main axon in these cells bifurcated within the dorsal grey matter and while one branch followed the regular path of PNs, the other one entered the dorsal funiculus and ascended there in the ipsilateral side. Lamina I PNs with collaterals crossing the midline at the supraspinal level and thus achieving bilateral projections have been reported before *(Al-Khater and Todd, 2009).* In case of the four bilateral projection neurons in our sample the splitting of the main axon occurs earlier and the two equally strong branches seemingly ascend in different tracts from the beginning.

Since LSN is known to project bilaterally to the mediodorsal thalamic nucleus *(Gauriau and Bernard 2004)*, it would be tempting to say that bilaterally projecting neurons may contribute to this double projection. However, from a metabolic point of view, bilateral projection this way would be very inefficient due to the high energy cost of maintaining the two branches. It is more likely that the ipsilateral branch is establishing long propriospinal connections on the ipsilateral side while the contralateral branch ascends to supraspinal targets.

Indeed, LSN neurons could be double labelled from two injection sites in the brain stem and diencephalon, as well as in the brainstem and spinal cord *(Réthelyi, 2003)*, which raised the possibility that these neurons probably take part in the establishment of propriospinal connections via collateral axon branches. Furthermore, when the retrograde tracer cholera toxin beta-subunit (CTB) was used to trace long ascending propriospinal projections from neurons in the lumbosacral spinal cord to the upper cervical grey matter some lumbosacral superficial dorsal horn neurons were identified. These propriospinal projections were suggested to be involved in coordinating head and neck movements during locomotion or stimulus-evoked motor responses *(Dutton et al., 2006)*. In addition, LSN neurons in the upper cervical segments can be labeled from the upper thoracic segments *(Verburgh et al., 1990).* Conversely, anterogradely labeled axons of the LSN neurons located in cervical segments have been detected around the neurons in the intermediolateral nucleus in the middle thoracic segments *(Jansen and Loewy, 1997).* This caudal propriospinal connection is supported by our finding that bilateral neurons in the LSN and outside the dorsal grey also issued long but thin caudal collaterals in the ipsilateral DLF or Lissauer-tract.

CONCLUSIONS

Our findings indicate that the widespread axonal arbor of lamina I LCNs and frequent collaterals in the dorsolateral white matter designate these neurons, besides some lamina I PNs, as candidates for establishing short- and long-range, intrasegmental and intersegmental propriospinal connections. We have demonstrated the existence of these theoretical propriospinal connections, from lamina I PNs and LCNs onto other lamina I and LSN neurons, which are not frequent but some are extremely potent. The latter may be important in sustained nociceptive signaling during pathological conditions.

We revealed unique axon trajectories of putative projection or propriospinal neurons in the lateral aspect of the dorsal horn and in the LSN that suggests a development different from the regular lamina I projection cells. While LSN is not present in all species the novel axon trajectories revealed in our study may help to identify cell groups with analogous function and developmental origin in other species.

Our findings emphasize the importance of understanding the connectivity matrix of the superficial dorsal horn in order to decipher spinal sensory information processing.

ÖSSZEFOGLALÁS

Kutatási eredményeink szerint az I-es lamina interneuronjainak axonja gyakran igen kiterjedt kollaterális hálózattal bír dorsolateralis fehérállományban és ebből következően, az I-es lamina egyes projekciós neuronjai mellett, potenciálisan alkalmasak rövid- és hosszútávú intraszegmentális és interszegmentális propriospinális kapcsolatok kialakítására. Elektrofiziológiai módszerekkel sikerült kimutatnunk ilyen propriospinális kapcsolatokat az I-es lamina projekciós neuronjai és interneuronjai valamint más I-es lamina illetve LSN sejt között. Annak ellenére, hogy ezen kapcsolatok nem gyakoriak, néhányuk kivételesen hatékonynak bizonyult. Ez utóbbi kapcsolatok külön jelentőséggel bírhatnak a pathológiás körülmények között jellemző módosult nociceptív transzmisszióban.

A fenti eredmények mellett, kutatásaink során egyedi axon lefutási mintázattal bíró, valószínűleg projekciós neuronokat azonosítottunk a felületes hátsó szarv laterális területén és az LSN-ben. Ezen újonnan leírt axon lefutási mintázatok eltérnek az I-es lamina területén korábban megfigyeltektől, és azoktól eltérő fejlődési útvonalakat feltételeznek. Bár az LSN nem található meg minden fajban, az általunk leírt jellegzetes axonlefutási minták segíthetnek azonosítani az LSN-nel azonos eredetű és analóg funkciójú neuroncsoportokat más fajokban, pl. az emberben.
Eredményeink hangsúlyozzák, hogy a gerincvelői szintű szenzoros információ feldolgozás folyamatának megfejtéséhez elengedhetetlen a felületes hátsó szarvi neuronhálózatok összeköttetéseinek megismerése és megértése.

KEY WORDS

spinal cord, dorsal horn, lateral spinal nucleus, dorsal horn circuitry, 3-D-reconstruction, projection neuron, local circuit neuron, axon trajectory

KULCSSZAVAK

gerincvelő, hátsó szarv, nucleus spinalis lateralis, hátsó szarvi neuronhálózatok, 3-D sejtrekonstrukció, projekciós neuron, interneuron, axon lefutási mintázat

ACKNOWLEDGEMENTS

I would like to express my deepest honor and gratitude to my supervisor, Péter Szücs for the scientific approach he conveyed to me. I am thankful to Professor Miklós Antal, and Professor Boris V. Safronov for making it possible for me to visit the laboratory of Spinal Neuronal Networks Research group in Porto, and to Liliana Luz and Raquel O. Pinho for their excellent and indisposed technical help in acquiring skills in paired electrophyiological recordings and histological processing.

Last, but not at all least, I'm unutterably grateful to my family, especially to my husband for his patience and support during my work.

My work was supported by TÁMOP-4.2.4.A/2-11/1-2012-0001 ***'National Excellence Program'*** *supported by the State of Hungary and the European Union, co-financed by the European Social Fund. and FEDER funds through the Operational competitiveness Programme – COMPETE and by national funds through FCT – Fundação para a Ciência e a Tecnologia under the project FCOMP-01-0124-FEDER-029632 (PTDC/NEU-SCC/0347/2012 to Boris Safronov),*

EXTERNAL REFERENCES

1. Al Ghamdi, K. S., Polgar, E. and Todd, A. J. (2009) Soma size distinguishes projection neurons from neurokinin 1 receptor-expressing interneurons in lamina 1 of the rat lumbar spinal dorsal horn. *Neuroscience*, **164**, 1794-1804.
2. Al-Khater, K. M. and Todd, A. J. (2009) Collateral projections of neurons in laminae I, III, and IV of rat spinal cord to thalamus, periaqueductal gray matter, and lateral parabrachial area. *Journal of Comparative Neurology*, **515**, 629-646.
3. Alvarez, F. J., Villalba, R. M., Carr, P. A., Grandes, P. and Somohano, P. M. (2000) Differential distribution of metabotropic glutamate receptor 1a, 1b and 5 in the rat spinal cord. *Journal of Comparative Neurology*, **422**, 464-487.
4. Andrew, D and Craig, A.D. (2002) Quantitative responses of spinothalamic lamina I neurones to graded mechanical stimulation in the cat. *Journal of Physiology*, **545**, 913-931.
5. Apkarin, A. V., Bushnell, M. C., Treede, R. D. and Zubieta, J. K. (2005) Human brain mechanisms of pain perception and regulation in health and diseae. *European Journal of Pain*, **9**, 463-484.
6. Augsburger, A., Schuchardt, A., Hoskins, S., Dodd, J. and Butler, S. (1999) BMPs as mediators of roof plate repulsion of commissural neurons. *Neuron*, **24**, 127-141.
7. Basbaum, A. I. (2009) Cellular and Molecular Mechanisms of Pain. *Cell*, **139**, 267-284.
8. Basbaum, A. I. and Bushnell M. C. (2009) *Science of Pain.Pain.* Academic Press, Oxford, San Diego.
9. Battaglia, G. and Rustioni, A. (1992) Substance P innervation of the rat and cat thalamus. II. Cells of origin in the spinal cord. *Journal of Comparative Neurology*, **315**, 473-486.
10. Bell, C. and Shaw, A. (1868) Reprint of the "idea of a New Anatomy of the Brain," with letters, &c. *Journal of Anatomy and Physiology,* **3**, 147-182.
11. Belmonte, C. and Cervero, F. (1996) *Neurobiology of nociceptors.* Oxford University Press, Oxford, New York.

12. Bergman, E., Carlsson, K., Liljeborg , A., Manders, E., Hokfelt, T. and Ulfhake, B. (1999) Neuropeptides, nitric oxide synthase and GAP-43 in B4-binding and RT97 immunoreactive primary sensory neurons: Normal distribution pattern and changes after peripheral nerve transection and aging. *Brain Research*, **832**, 63-83.

13. Bernard, J. F., Dallel, R., Raboisson, P., Villanueva, L. and Le Bars, D. (1995) Organization of the efferent projections from the spinal cervical enlargement to the parabrachial area and the periaqueductal gray: a PHA-L study in the rat. *Journal of Comparative Neurology*, **353**, 480-505.

14. Braz, J. M. and Basbaum, A. I. (2009) Triggering genetically-expressed transneuronal tracers by peripheral axotomy reveals convergent and segregated sensory neuron-spinal cord connectivity. *Neuroscience*, **163**, 1220-1232.

15. Braz, J., Solorzano, C., Wang, X. and Basbaum A. I. (2014) Transmitting pain and itch messages: a contemporary view of the spinal cord circuits that generate gate control. *Neuron,* **82**, 522-536.

16. Bresnahan, J. C., Ho, R. H. and Beattie, M. S. (1984) A comparison of the ultrastructure of substance P and enkephalin-immunoreactive elements in the nucleus of the dorsal lateral funiculus and laminae I and II of the rat spinal cord. *Journal of Comparative Neurology*, **229**, 497-511.

17. Brown, J. L., Liu, H., Maggio, J. E. Vigna, S. R., Mantyh, P. W. and Basbaum, A. I. (1995) Morphological characterization of substance P receptor-immunoreactive neurons in rat spinal cord and trigeminal nucleus caudalis. *Journal of Comparative Neurology*, **356**, 327-344.

18. Burstein, R. and Giesler Jr., G. J. (1989) Retrograde labeling of neurons in spinal cord that project directly to nucleus accumbens or the septal nuclei in the rat. *Brain Research*, **497**, 149-154.

19. Burstein, R. and Potrebic, S. (1993) Retrograde labeling of neurons in the spinal cord that project to the amygdala or the orbital cortex in the rat. *Journal of Comparative Neurology*, **335**, 469-485.

20. Burstein, R., Cliffer, K. D. and Giesler Jr. G. J. (1990) Cells of origin of the spinohypothalamic tract in the rat. *Journal of Comparative Neurology*, **291**, 329-344.

21. Cajal, Y. R. (1909) *Histologie du systéme nerveux.* Maloine, Paris.

22. Carlton, S. M., Chung, J. M., Leonard, R. B. and Willis, W. D. (1985) Funicular trajectories of brainstem neurons projectin to the lumbar spinal cord in the monkey (Macaca fascicularis): a retrograde labeling study. *Journal of Comparative Neurology,* **241**, 382-404.

23. Carr, P. A., Yamato, T. and Nagy, J. I. (1990) Calcitonin gene-related peptide in primary afferent neurons of rat: Co-existence with fluoride-resistant acid phosphatase and depletion by neonatal capsaicin. *Neuroscience*, **36**, 751-760.

24. Cavanaugh, D. J., Lee, H., Lo, L., Shields, S. D., Zylka, M. J., Basbaum, A. I. and Anderson, D. J. (2009) Distinct subset of unmyelinated primary sensory fibers mediate behavioral responses to noxious thermal and mechanical stimuli. *Proceedings in the National Academy of Sciences*, **106**, 9075-9080.

25. Cervero, F., Iggo, A. and Molony, V. (1979) Ascending projections of nociceptor-driven lamina I neurones in the cat. *Experimental Brain Research,* **35,** 135-149.

26. Charron, F., Stein, E., Jeong, J., McMahon, A. P. and Tessier-Lavigne, M. (2003) The morphogen sonic hedgehog is an axonal chemoattractant that collaborates with netrin-1 in midline axon guidance. Cell, **113**, 11-23.

27. Chen, Z., Gore, B. B., Long, H., Ma, L., Tessier-Lavigne, M. (2008) Alternative splicing of the Robo3 axon guidance receptor governs the midline switch from attraction to repulsion. *Neuron*, **58**, 325-332.

28. Cliffer, K. D., Urca, G., Elde, R. P. and Giesler, G. J. (1988) Studies of peptidergic input to the lateral spinal nucleus. *Brain Research*, **460**, 356-360.

29. Conrath, M., Taquet, H., Pohl, M. and Carayon, A. (1989) Immunocytochemical evidence for calcitonin gene-related peptide-like neurons in the dorsal horn and lateral spinal nucleus of the rat cervical spinal cord. *Journal of Chemical Neuroanatomy*, **2**, 335-347.

30. Craig, A. D. (2003) Pain mechanisms: labeled lines versus convergence in central processing. *Annual review of Neuroscience*, **26**, 1-30.

31. Dahlhaus, A., Ruscheweyh, R. and Sandkühler, J. (2005) Synaptic input of rat spinal lamina I projection and unidentified neurones in vitro. *Journal of Physiology,* **566,** 355-368.

32. Davidoff, R. A. (1984) *Handbook of the spinal cord. Synaptic connectivity in the spinal dorsal horn.* Dekker, New York.

33. Debanne, D., Campanac, E., Bialowas, A., Carlier E., Alcaraz, G. (2011) Axon physiology. *Physiological reviews*, **91**, 555-602.

34. Ding, Y. Q., Takada, M, Shigemoto, R and Mizumo, N. (1995) Spinoparabrachial tract neurons showing substance P receptor-like immunoreactivity in the lumbar spinal cord of the rat. *Brain Research*, **674**, 336-340.

35. Dubner, R. and Ruda, M. A. (1992) Activity-dependant neuronal plasticity following tissue injury and inflammation. *Trends in Neurosciences,* **15**, 96-103.

36. Dubner, R., Kenshalo, D. R., Maixner, W., Bushnell, M. C. and Oliveras, J. L. (1989) The correlation of monkey medullary dorsal horn neuronal activity and the percieved intensity of noxious heat stimuli. *Journal of Neurophysiology*, **62**, 450-457.

37. Dutton, R. C., Carstens, M. I., Antognini, J. F. and Carstens, E. (2006) Long ascending propriospinal projections from lumbosacral to upper cervical spinal cord in the rat. *Brain Research*, **1119**, 76-85.

38. Eckert, W. A 3rd, McNaughton, K. K. and Light, A. R. (2003) Morphology and axonal arborization of rat spinal inner lamina II neurons hyperpolarized by mu-opioid selective agonists. *Journal of Comparative Neurology*, **458**, 240-256.

39. Edwards, F. A., Konnerth, A., Sakmann, B. and Takahashi, T. (1989) A thin slice preparation for patch clamp recordings from neurones of the mammalian central nervous system. *Pflügers Archiv European Journal of Physiology*, **414**, 600-612.

40. Escalante, A., Murillo, B., Morenilla-Palao, C., Klar, A. and Herrera, E. (2013) Zic2-dependent axon midline avoidance controls the formation of major ipsilateral tracts in the CNS. *Neuron,* **80**, 1392-1406.

41. Esteves, F., Lima, D. and Coimbra, A. (1993) Structural types of spinal cord marginal (lamina I) neurons projecting to the nucleus of the tractus solitarius of the rat. *Somatosensory & Motor Research*, **10**, 203-216.

42. Feil, K. and Herbert, H. (1995) Topographic organization of spinal and trigeminal somatosensory pathways to the rat parabrachial and Kölliker-Fuse neclei. *Journal of Comparative Neurology*, **353**, 506-528.

43. Fürst, Zs. (2006) *Farmakológia.*. Medicina, Budapest.

44. Gauriau, C. and Bernard, J.F. (2004) A comparative reappraisal of projections from the superficial dorsal horn in the rat: the forebrain. *Journal of Comparative Neurology*, **468**, 24-56.

45. Giesler Jr., G. J., Urca, G, Cannon, J. T. and Liebeskind, J. C. (1979) Response properties of neurons of the lateral cervical nucleus in the rat. *Journal of Comparative Neurology*, **186**, 65-77.

46. Giesler, G. J. and Elde, R. P. (1985) Immunocytochemical studies of the peptidergic fibers and terminals within the lateral spinal and lateral cervcal nuclei. *Journal of Neuroscience*, **5**, 1833-1841.

47. Gobel, S. (1978) Golgi studies of the neurons in layer I of the dorsal horn of the medulla (trigeminal nucleus caudalis). *Journal of Comparative Neurology*, **180**, 375-394.

48. Grudt, T. J. and Perl, E. R. (2002) Correlations between neuronal morphology and electrophysiological features in the rodent superficial dorsal horn. *Journal of Physiology*, **540**, 189-207.

49. Gwny, D. G. and Waldron, H. A. (1969) Observations on the morphology of a nucleus in the dorsolateral funiculus of the spinal cord of the guinea-pig, rabbit, ferrat and cat. *Journal of Comparative Neurology*, **136**, 233-236.

50. Gwyn, D. G. and Waldron, H. A. (1968) A nucleus in the dorsolateral funiculus of the spinal cord of the rat. *Brain Research*, **10**, 342-351.

51. Han, Z. S., Zhang, E. T. and Craig, A. D. (1998) Nociceptive and thermoreceptive lamina I neurons are anatomically distinct. *Nature Neuroscience*, **1**, 218-225.

52. Handwerker, H. O. and Kobal, G. (1993) Psychophysiology of experimentally induced pain. *Physiological rewievs*. **73**, 639-671.

53. Harmann, P. A., Carlton, S. M. and Willis, W. D. (1988) Collaterals of spinothalamic tract cells to the periaqueductal gray: a fluorescent double-labeling study in the rat. *Brain Research* **441**, 87-97.

54. Harper, A. A. and Lawson, S. N. (1985) Conduction velocity is related to morphological cell type in rat dorsal root ganglion neurones. *Journal of Physiology*, **359**, 31-46.

55. Hökfelt, T., Ljungdahl, A., Terenius, L., Elde, R. and Nilsson, G. (1977) Immunohistochemical analysis of peptide pathways possibly related to pain and analgesia: enkephalin and substance P. *Proceedings of the National Academy of Sciences*, **74**, 3081-3085.

56. Hunt, S. P., and Rossi, J. (1985) Peptide- and non-peptide-containing unmyelinated primary afferents: The parallel processing of nociceptive information. *Philosophical Transactions of the Royal Society B*, **308**, 283-289.

57. Ikeda, H., Heinke, B., Ruscheweyh, R. and Sandkühler, J. (2003) Synaptic plasticity in spinal lamina I projection neurons that mediate hyperalgesia. *Science*, **299**, 1237-1240.

58. Jansen, A. S. and Loewy, A. D. (1997) Neurons lying in the white matter of the upper cervical spinal cord project to the intermediolateral cell coloumn. *Neuroscience*, **77**, 889-898.

59. Jiang, M. C., Liu, L. and Gebhart, G. F. (1999) Cellular properties of lateral spinal nucleus neurons in the rat L6-S1 spinal cord. *Journal of Neurophysiology*, **81**, 3078-3086.

60. Julius , D., and Basbaum, A. I. (2001) Molecular mechanisms of nociception. *Nature,* **413**, 203-210.

61. Kashiba, H., Uchida Y. and Senba, E. (2001) Difference in binding by isolectin B4 to trkA and c-ret mRNA-expressing neurons in rat sensory ganglia. *Molecular Brain Research*, **95**, 18-26.

62. Kato, G., Kawasaki, Y., Koga, K., Uta, D., Kosugi, M., Yasaka, T., Yoshimura, M., Ji, R. R. and Strassman, A. M. (2009) Organization of intralaminar and translaminar neuronal connectivity in the superficial spinal dorsal horn. *Journal of Neuroscience,* **29**, 5088-5099.

63. Kennedy, T. E., Serafini, Z., de la Torre J. R. and Tessier-Lavigne, M. (1994) Netrins are diffusible chemotropic factors for commissural axons in the embryonic spinal cord. *Cell,* **78**, 425-435.

64. Knowlton, W. M., Palkar, R., Lippoldt, E. K. and McCoy, D. D. (2013) A sensory-labeled line for cold: TRPM8-expressing sensory neurons define

the cellular basis for cold, old pain, and cooling mediated analgesia. *Journal of Neuroscience*, **33**, 2837-2848.

65. Koltzenburg, M. (1995) Stability and plasticity of nociceptor function and their relationship to provoked and ongoing pain. *Seminars in Neuroscience*, **7**, 199-210.

66. Lawson, S. N. and Waddell, P. J. (1991) Soma neurofilament immunreactivity is related to cell size and conduction velocity in rat primary sensory neurons. *Journal of Physiology*, **435**, 41-63.

67. Leah, J., Menetrey, D. and De-Pommery, J. (1988) Neuropeptides in long ascending spinal tract cells in the rat: evidence for parallel processing of ascending information. *Neuroscience*, **24**, 195-207.

68. Lee, D. C., Jensen, A. L., Schiefer, M. A., Morgan, C. W. and Grill, W. M. (2005) Structural mechanisms to produce differential dendritic gains. *Brain Research,* **1033**, 117-127.

69. Lenhossék, M. (1895) *Der feinere Bau des Nervensystems im Lichte neuester Forschungen. Eine allgemeine Betrachtung der Strukturprincipien des Nervensystems, nebst einer Darstellung des feineren Baues des Rückenmarkes.* Kornfeld, Berlin.

70. Li, J. L., Ding, Y. Q., Shigemoto, R and Mizuno, N (1996) Distribution of trigeminothalamic and spinothalamic-tract neurons showing substance P receptor-like immunoreactivity in the rat. *Brain Research*, **719**, 207-212.

71. Li, Y. Q., Li, H., Yang, K., Kaneko, T. and Mizuno, N. (2000) Morphologic features and electrical membrane properties of projection neurons in the marginal layer of the medullary dorsal horn of the rat. *Journal of Comparative Neurology,* **424**, 24-36.

72. Light, A. R. (1992) *Pain and Headache: the Initial Processing of Pain and its Descending Control: Spinal and Trigeminal Systems*. Karger, Basel.

73. Light, A. R. and Kavookijan, A. M. (1988) Morphology and ultrastructure of physiologically identified substantia gelatinosa (lamina II) neurons with axons that terminate in deeper laminae (III-V). *Journal of Comparative Neurology,* **267**, 172-189.

74. Light, A. R. and Willcockson, H. H. (1999) Spinal laminae I-II neurons in rat recorded in vivo in whole cell, tight seal configuration: properties and opioid responses. *Journal of Neurophysiology,* **82,** 3316-3326.

75. Light, A. R., Trevino, D. L., and Perl, E. R. (1979) Morphological features of functionally defined neurons in the marginal one and substantia gelatinosa of the spinal dorsal horn. *Journal of Comparative Neurology*, **186**, 151-171.

76. Lima, D. (1998) Anatomical basis for the dynamic processing of nociceptive input. *European Journal of Neuroscience*, **24**, 195-207.

77. Lima, D. and Coimbra, A. (1983) The neuronal population of the marginal zone (lamina I) of the rat spinal cord. A study based on reconstructions of serially sectioned cells. *Anatomy and Embryology*, **167**, 273-288.

78. Lima, D. and Coimbra, A. (1986) A Golgi study of the neuronal population of the maginal zone (lamina I) of the rat spinal cord. *Journal of Comparative Neurology,* **244**, 53-71.

79. Littlewood, N. K., Todd, A. J., Spike, R. C., Watt, C. and Shehab, S. A. (1995) The types of neuron in spinal dosal horn which possess neurokinin-1 receptors. *Neuroscience*, **66**, 597-608.

80. Long, H., Sabatier, C., Ma, L., Plump, A., Yuan, W., Ornitz, D. M., Tamada, A. Murakami, F., Goodman, C., S. and Tessier-Lavigne, M. (2004) Conserved roles for Slit and Robo proteins in midline comissural axon guidance. *Neuron,* **42,** 213-223.

81. Lu, Y. and Perl, E. R. (2003) A specific inhibitory pathway between substantia gelatinosa neurons recieveng direct C-fiber input. *Journal of Neuroscience,* **23**, 8752-8758.

82. Lu, Y. and Perl, E. R. (2005) Modular organization of excitatory circuits between neurons of the spinal superficial dorsal horn (laminae I and II). *Journal of Neuroscience*, **25**, 3900-3907.

83. Luz, L. L., Szücs, P. and Safronov, B. V. (2014) Peripherally driven low-threshold inhibitory inputs to lamina I local circuit and projection neurones: a new circuit for gating pain responses. *Journal of Physiology*, **592**, 1519-1534.

84. Luz, L. L., Szucs, P., Pinho, R. and Safronov, B. V. (2010) Monosyanptic excitatory inputs to spinal lamina I anterolateral-tract-projecting neurons from neighbouring lamina I neurons. *Journal of Physiology*, **588**, 4489-4505.

85. Marshall, G. E., Shehab, S. A., Spike, R. C. and Todd, A. J. (1996) Neurokinin-1 receptors on lumbar spinothalamic neurons in the rat. *Neruoscience*, **72**, 255-263.

86. Masson Jr., R. L., Sparkes, M. L. and Ritz, L. A. (1991) Descending projections to the rat sacrocaudal spinal cord. *Journal of Comparative Neurology*, **307**, 120-130.

87. Maxwell, D. J., Belle, M. D., Cheunsuang, O., Stewart, A. and Morris, R. (2007) Morphology of inhibitory and excitatory interneurons in superficial laminae of the rat dorsal horn. *Journal of Physiology*, **584**, 521-533.

88. McMahon, S. B. and Koltzenburg, M. (2006) *Wall and Melzack's Textbook of Pain. Section 1. Neurobiology of pain.* Elsevier, Churchill Livingstone.

89. Melzack, R. and Wall, P. D. (1965) Pain mechanisms: a new theory. *Science*, **150**, 971-979.

90. Kenshalo, D. R. (1968) *The skin senses*. Thomas, Springfield,

91. Menetrey, D. and Basbaum, A. I. (1987) Spinal and trigeminal projections to the nucleus of the solitary tract: a possible substrate for somatovisceral and viscerovisceral reflex activation. *Journal of Comparative Neurology*, **255**, 439-450.

92. Menétrey, D., Chaouch, A. and Besson, J. M. (1980) Location and properties of dorsal horn neurons at origin of spinoreticular tract in lumbar enlargement of the rat. *Journal of Neurophysiology*, **44**, 862-877.

93. Menetrey, D., Chaouch, A., Binder, D. and Besson, J. M. (1982) The origin of the spinomesencephalic tract in the rat: An anatomical study using the retrograde transport of horseradish peroxidase. *Journal of Comparative Neurology*, **206**, 193-207.

94. Mense, S. (1993) Nociception from skeletal muscle in relation to clinical muscle pain. *Pain*, **54**, 241-289.

95. Mesnage, B., Gaillard, S., Godin, A. G., Rodeau, J. L., Hammer, M., Von Engelhardt, J., Wiseman, P. W., De Koninck, Y., Schlichter, R., Cordero-Erausquin, M. (2011) Morphological and functional characterization of cholinergic interneurons in the dorsal horn of the mouse spinal cord. *Journal of Comparative Neurology*, **519**, 3139-3158.

96. Millan, M. J. (1998) The induction of pain: an integrative review. Progress in Neurobiology, **57**, 1-164.

97. Millan, M. J. (2002) Descending control of pain. *Progress in Neurobiology*, **66**, 355-474.

98. Nagy, J. I. and Hunt, S. P. (1982) Fluoride-rsistant acid phosphatase-containing neurones in dorsal root ganglia are separate from those containing substance P or somatostatin. *Neuroscience*, **7**, 89-97.

99. Nahin, R. L. (1987) Immunocytochemical identification of long ascending peptidergic neurons contributing to the spinoreticular tract in the rat. *Neuroscience*, **23**, 859-869.

100. Ness, T. J. and Gebhart, G. F. (1990) Visceral pain: a review of experimental studies. *Pain*, **41**, 167-234.

101. Nissl, F. (1894) Über die sogennanten Granula der Nervenzellen. *Neurol. Zbl*., **13**, 676-685.

102. Olave, M. J. and Maxwell, D. J. (2004) Axon terminals possessing α_{2c} – adrenergic receptors densely innervate neurons in the rat lateral spinal nucleus which respond to noxious stimulation. *Neuroscience*, **126**, 391-403.

103. Pechura, C. M. and Liu, R. P. (1986) Spinal neurons which project to the periaqueductal gray and the medullary reticular formation via axon collaterals: a double label fluorescence study in the rat. *Brain Research*, **374**, 357-361.

104. Perl, E. R. (2007) Ideas about pain, a historical view. *Nature Reviews Neuroscience,* **8**, 71-80.

105. Petkó, M. and Antal, M. (2000) Propriospinal afferent and efferent connections of the lateral and medial areas of the dorsal horn (laminae I-IV) in the rat lumbar spinal cord. *Journal of Comparative Neurology*, **422,** 312-325.

106. Petkó, M., Veress, G., Vereb, Gy., Storm-Mathiesen, J. and Antal, M. (2004) Commissural propriospinal connections between the lateral aspects of laminae III-IV in the lumbar spinal cord of rats. *Journal of Comparative Neurology,* **480**, 364-377.

107. Pinto, V., Derkach, V. A. and Safronov, B. V. (2008*a*) Role of TTX-sensitive and TTX-resistant sodium channels in Adelta- and C-fiber

conduction and synaptic transmission. *Journal of Neurophysiology,* **99**, 617-628.

108. Pinto, V., Szűcs, P., Derkach, V. A. and Safronov, B. V. (2008*b*) Monosynaptic convergence of C- and Adelta-afferent fibers from different segmental dorsal roots on to single substantia gelatinosa neurones in the rat spinal cord. *Journal of Physiology*, **586**, 4165-4177.
109. Pinto, V., Szücs, P., Lima, D. and Safronov, B. V. (2010) Multisegmental Aδ- and C-fiber input to neurons in lamina I and the lateral spinal nucleus. *Journal of Neuroscience*, **30**, 2384-2395.
110. Polgar, E., Al-Khater, K. M. , Shehab, S, Watanabe, M. and Todd, A. J. (2008) Large projection neurons in lamina I of the rat spinal cord that lack the neurokinin 1 receptor are densely innervated by VGLUT2-containing axons and possess GluR4-containing AMPA receptors. *Journal of Neuroscience*, **28**, 13150-13160.
111. Polgar, E., Puskar, Z., Watt, C., Matesz, K. and Todd, A. J. (2002) Selective innervation of lamina I projection neurons that possess the neurokinin I receptor by serotonin-containing axons in the rat spinal cord. *Neuroscience*, **109**, 799-809.
112. Puskar, Z., Polgar, E. and Todd., A. J. (2001) A population of large lamina I neurons with selective inhibitory input in rat spinal cord. *Neuroscience*, **102**, 167-176.
113. Reed, W.R., Shum-siu A., Onifer, S. M. and Magnuson, D. S. K. (2006) Inter-enlargement pathways in the ventrolateral funiculus of the adult rat spinal cord. *Neuroscience* **142**, 1195-1207.
114. Reeh, P. W., Bayer, J., Kocher, L. and Handwerker, H. O. (1987) Sensitization of nociceptive cutaneous nerve fibers from the rat tail by noxious mechanical stimulation. *Experimental Brain Research*, **65**, 505-512.
115. Réthelyi M. (2002) *Funkcionális Anatómia.* Medicina, Budapest
116. Réthelyi, M. (2003) Neurons of the lateral spinal nucleus in the rat spinal cord – A Golgi study. *European Journal of Anatomy*, **7**, 1-8.
117. Rexed, B. (1952) The cytoarchitectonic organization of the spinal cord in the cat. *Journal of Comparative Neurology*, **96**, 414-495.

118. Sabatier, C., Plump, A. S., Le, M., Brose, K., Tamada, A., Murakami, F., Lee, E. Y. and Tessier-Lavigne, M. (2004) The divergent Robo family protein rig-1/Robo3 is a negative regulator of slit responsiveness required for midline crossing by commissural axons. *Cell*, **117**, 157-169.

119. Safronov, B. V., Pinto, V. and Derach, V. A. (2007) High-resolution single-cell imaging for functional studies in the whole brain and spinal cord and thick tissue blocks using light-emitting diode illumination. *Journal of Neuroscience Methods*, **164**, 292-298.

120. Santos, S. F. A., Rebelo, S., Derkach, V. A. and Safronov, B. V. (2007) Excitatory interneurons dominate sensory processing in the spinal substantia gelatinosa of rat. *Journal of Physiology,* **581**, 241-254.

121. Santos, S. F. A., Luz, L. L., Szucs, P., Lima, D., Derkach, V. A., Safronov, B. V. (2009) Transmission efficacy and plasticity in glutamatergic synapses formed by excitatory interneurons of the substantia gelatinosa in the rat spinal cord. *PLoS One,* **4**, e8047.

122. Seybold, V. and Elde, R. (1980) Immunohistochemical studies of peptideric neurons in the dorsal horn of the spinal cord. *Journal of Histochemistry & Cytochemistry,* **28**, 367-370.

123. Sherrington, C. S. (1906) *The Integrative Action of the Nervous System.* Yale University Press, New Haven.

124. Silverman, J. D. and Kruger, L. (1988) Acid phosphatase as a selective marker for a class of small sensory ganglion cells in several mammals: Spinal cord distribution, histochemical properties, and relation to fluoride-resistant acid phosphatase (FRAP) of rodents. *Somatosensory & motor research*, **5**, 219-246.

125. Silverman, J. D. and Kruger, L. (1989) Calcitonine-gene-related peptide-immunoreactive innevation of the rat head with emphasis on specialized sensory structures. *Journal of Comparative Neurology*, **280**, 303-330.

126. Simone, D. A. and Kajander, K. C. (1997) Responses of cutaneous A-fiber nociceptors to noxious cold. *Journal of Neurophysiology*, **77**, 2049-2060.

127. Sinclair, D. C. (1955) Cutaneous sensation and the doctrine of specific energy. *Brain*, **78**, 584-614.

128. Snider, W. D., and McMahon, S. B. (1998). Tackling pain at the source: new ideas about nociceptors. *Neuron,* **20**, 629-632.

129. Spike, R. C. a, Todd, A. J. and Johnston, H. M. (1993) Coexistence of NADPH diaphorase with GABA, glycine and acetylcholine in rat spinal cord. *Journal of Comparative Neurology*, **335**, 320-333.

130. Spike, R. C., Puskar, Z. and Todd, A. J. (2003) A quantitative and morphological study of projection neurons in lamina I of the rat lumbar spinal cord. *European Journal of Neuroscience*, **18**, 2433-2448.

131. Sugiura, Y., Terui, N. and Hosoya, Y. (1989) Difference in distribution of central terminals between visceral and somatic unmyelinated (C) primary afferent fibers. *Journal of Neurophysiology*, **62**, 834-840.

132. Szentágothai J. (1964) Neuronal and Synaptic Arrangement in the Substantia Gelatinosa Rolandi. *Journal of Comparative Neurolology*, **122**, 219-239.

133. Szirmai, I. (2006) *Neurológia.* Medicina, Budapest.

134. Szücs, P., Luz, L. L., Lima, D. and Safronov, B. V. (2010) Local axon collaterals of lamina I projection neurons in the spinal cord of young rats. *Journal of Comparative Neurology*, **518**, 2645-2665.

135. Szücs, P., Pinto, V. and Safronov, B: V. (2009) Advanced technique of infrared LED imaging of unstained cells and intracellular structures in isolated spinal cord, brain stem, ganglia and cerebellum. *Journal of Neuroscience Methods,* **177**, 369-380.

136. Thome, C., Kelly, T., Yanez, A., Schultz, C., Engelhardt, M., Cambridge, S. B., Both, M., Draguhn, A., Beck, H. and Egorov, A. V. (2014) Axon-carrying dendrites convey privileged synaptic input in hippocampal neurons. *Neuron*, **83**, 1418-1430.

137. Todd, A. J. (2010) Neuronal circuitry for pain processing in the dorsal horn. *Nature Reviews Neuroscience,* **11**, 823-836.

138. Todd, A. J. and McKenzie, J. (1989) GABA-immunoreactive neurons in the dorsal horn of the rat spinal cord. *Neuroscience*, **31**, 799-806.

139. Todd, A. J. and Spike, R. C. (1993) The localization of classical transmitters and neuropeptides within neurons in laminae I-III of the mammalian spinal dorsal horn. *Progress in Neurobiology*, **41**, 609-646.

140. Todd, A. J. and Sullivan, A. C. (1990) Light microscope study of coexistence of GABA-like and glycine-like immunoreactivities in the spinal cord of the art. *Journal of Comparative Neurology*, **296**, 496-505.

141. Todd, A. J., Puskar, Z., Spike, R. C., Hughes, C., Watt, C. and Forrest, L. (2002) Projection neurons in lamina I of rat spinal cord with the neurokinin I receptor are selectively innervated by substance P-containing afferents and respond to noxious stimulation. *Journal of Neuroscience,* **22**, 4103-4113.

142. Todd, A. J., Spike, R. C., Price, R. F. and Neilson, M. (1994) Immunocytochemical evidence that neurotensin is present in glutamatergic neurons in the superficial dorsal horn of the rat. *Journal of Neuroscience*, **14**, 774-784.

143. Treede, R. D. and Magerl., W. (1995) Modern concepts of pain and hyperalgesia: beyond the polymodal C nociceptor. *News in Physiological Sciences*, **10**, 216-228.

144. Verburgh, C. A., Voogd, J., Kuypers, H. G. and Stevens, H. P. (1990) Propriospinal neurons with ascending collaterals to the dorsal medulla, the thalamus and the tectum: a retrograde fluorescent double-labeling study of the cervical cord of the rat. *Experimental Brain Research*, **80**, 577-590.

145. Wang, H., Riveiro-Melian, C., Robertson, B., and Grant, G. (1994) Transganglionc transport and binding of the isolectin IB4 from Griffiona simplicifolia I in rt primary sensory neurons. *Neuroscience*, **62**, 539-552.

146. Weddel, G. (1955) Somesthesis and the chemical senses. *Annual Review of Psychology*, **6**, 119-136.

147. Willis, W. D. and Coggeshall R. E. (2004*) Sensory Mechanisms of the Spinal Cord. Vol. 1. Sensory Receptors and Peripheral Nerves.* Kluwer Academic/Plenum Publishers, New York.

148. Yasaka, T, Tiong, S. Y., Hughes, D. I., Riddel, J. S. and Todd, A. J. (2010) Populations of inhibitory and excitatory interneurons in lamina II of the adult rat spinal dorsal horn revealed by a combined electrophysiological and anatomical approach. *Pain*, **151**, 475-488.

149. Zeilhofer, H. U., Wildner, H and Yévenes, G., E. (2012) Fast synaptic inhibition in spinal sensory processing and pain control. *Physiological reviews*, **92**, 193-235.

150. Zhang, E. T. and Craig, A. D. (1997) Morphology and distribution of spinothalamic lamina I neurons in the monkey. *Journal of Neuroscience*, **17**, 3274-3284.

151. Zhang, E. T., Han, Z. S. and Craig, A. D. (1996) Morphological classes of spinothalamic lamina I neurons in the cat. *Journal of Comparative Neurology,* **367**, 537-549.

152. Zou, Y., Stoeklyi, E., Chen, H. and Tessier-Lavigne, M. (2000) Squeezing axons out of gray matter: a role for slit and semaphorin proteins from midline and ventral spinal cord. *Cell*, **102**, 363-375.

SUPPLEMENT: LIST OF PUBLICATIONS

UNIVERSITY OF DEBRECEN
UNIVERSITY AND NATIONAL LIBRARY

Registry number: DEENK/85/2015.PL
Subject: Ph.D. List of Publications

Candidate: Zsófia Antal
Neptun ID: Z6HJML
Doctoral School: Doctoral School of Neurosciences
MTMT ID: 10034814

List of publications related to the dissertation

1. **Antal, Z.**, Luz, L.L., Safronov, B.V., Antal, M., Szűcs, P.: Neurons in the lateral part of the lumbar spinal cord show distinct novel axon trajectories and are excited by short propriospinal ascending inputs.
   Brain Struct. Funct. "accepted by publisher" (2015)
   IF:4.567 (2013)

2. Szűcs, P., Luz, L., Pinho, R., Aguiar, P., **Antal, Z.**, Tiong, S., Todd, A.J., Safronov, B.: Axon diversity of lamina I local-circuit neurons in the lumbar spinal.
   J. Comp. Neurol. 521 (12), 2719-2741, 2013.
   IF:3.508

Address: 1 Egyetem tér, Debrecen 4032, Hungary Postal address: Pf. 39. Debrecen 4010, Hungary
Tel.: +36 52 410 443 Fax: +36 52 512 900/63847 E-mail: publikaciok@lib.unideb.hu, ¤ Web: www.lib.unideb.hu

List of other publications

3. **Antal, Z.**, Szűcs, P., Antal, M.: Lamotrigine effectively blocks synaptic transmission between nociceptive primary afferents and secondary sensory neurons in the rat superficial spinal dorsal horn.
Interv. Med. Applied. Sci. 3 (1), 22-26, 2011.
DOI: http://dx.doi.org/10.1556/IMAS.3.2011.1.5

4. Papachatzaki, M.M., **Antal, Z.**, Terzi, D., Szűcs, P., Zachariou, V., Antal, M.: RGS9-2 modulates nociceptive behaviour and opioid-mediated synaptic transmission in the spinal dorsal horn.
Neurosci. Lett. 501 (1), 31-34, 2011.
DOI: http://dx.doi.org/10.1016/j.neulet.2011.06.033
IF:2.105

Total IF of journals (all publications): 10,18
Total IF of journals (publications related to the dissertation): 8,075

The Candidate's publication data submitted to the iDEa Tudóstér have been validated by DEENK on the basis of Web of Science, Scopus and Journal Citation Report (Impact Factor) databases.

16 April, 2015